Journal of Controlled Release 241 (2016) 200–219

Contents lists available at ScienceDirect

Journal of Controlled Release

journal homepage: www.elsevier.com/locate/jconrel

Review article

Functionalised carbon nanotubes: From intracellular uptake and cell-related toxicity to systemic brain delivery

Pedro M. Costa [1], Maxime Bourgognon [1], Julie T-W Wang, Khuloud T. Al-Jamal *

Institute of Pharmaceutical Science, Faculty of Life Sciences & Medicine, King's College London, Franklin—Wilkins Building, London SE1 9NH, United Kingdom

ARTICLE INFO

Article history:
Received 15 July 2016
Received in revised form 24 September 2016
Accepted 26 September 2016
Available online 30 September 2016

Keywords:
Carbon nanotubes (CNTs)
Functionalisation
Biocompatibility
Cell toxicity
Blood-brain barrier (BBB)
Brain delivery

ABSTRACT

Carbon nanotubes (CNTs) have long been regarded as promising carriers in biomedicine. Due to their high surface area and unique needle-like structure, CNTs are uniquely equipped to carry therapeutic molecules across biological membranes and, therefore, have been widely researched for use in theranostic applications. The attractive properties of the CNTs entice also their use in the brain environment. Cutting edge brain-specific therapies, capable of circumventing the physical and biochemical blockage of the blood-brain barrier, could be a precious tool to tackle brain disorders. With an increasing number of applications and expanding production, the effects of direct and indirect exposure to CNTs on cellular and molecular levels and more globally the general health, must be carefully assessed and limited.

In this chapter, we review the most recent trends on the development and application of CNT-based nanotechnologies, with a particular focus on the carrier properties, cell internalisation and processing, and mechanisms involved in cell toxicity. Novel approaches for CNT-based systemic therapeutic brain delivery following intravenous administration are also reviewed. Moreover, we highlight fundamental questions that should be addressed in future research involving CNTs, aiming at achieving its safe introduction into the clinics.

Contents

* Corresponding author at: Faculty of Life Sciences & Medicine, King's College London, Franklin—Wilkins Building, London SE1 9NH, United Kingdom.
E-mail address: khuloud.al-jamal@kcl.ac.uk (K.T. Al-Jamal).

[1] Shared equal contribution.

http://dx.doi.org/10.1016/j.jconrel.2016.09.033

1. Introduction

Carbon nanotubes (CNTs) are defined as cylindrical nanomaterials composed of a continuous, unbroken hexagonal mesh of carbon atoms. The first observation of CNTs by electron microscopy, credited to Iijima in 1991, opened a plethora of applications for this material [1]. This included not only high-strength composites, energy storage, and field emission device, but also the use of CNTs for biomedical applications [2]. In particular, CNT ability to cross efficiently cell membranes and carry a large amount of molecules has encouraged the design of nanotube-based delivery systems [3,4].

The concept of drug delivery was probably introduced by Paul Ehrlich, in 1897, when he theoreticized the use of "zauberkugeln" (in English "magic bullets") intending to improve the efficacy of available therapeutics [5]. Long after this statement, delivery of therapeutic and imaging agents into specific organs or tissues has remained a promising approach to modulate the pharmacokinetics and bioavailability of therapeutics, and provide controlled release kinetics at a target site. Numerous materials with sizes between 10 and 1000 nm have been investigated, including liposomes, dendrimers, nanoemulsions, nanoparticles, quantum dots and CNTs. With their needle-like shape, CNTs display singular physico-chemical properties. Their large surface area, ranging from 50 to 1315 m^2/g, allows the conjugation with extensive amount of therapeutic and imaging molecules [6–8]. Moreover, the high CNT length-to-diameter ratio enables them to efficiently penetrate biological membranes and accumulate into intracellular compartments [9]. Consequently, attachment of molecules to CNTs helps overcoming several administration problems, including insolubility, poor biodistribution and inability of therapeutic or diagnostic molecules to cross cellular barriers [3].

Despite their undeniable potential, concerns have emerged regarding the toxicity of CNTs, as various reports showed that pristine nanotubes could induce biological damage [10]. Excessive nanotube length, the presence of impurities from the synthesis process and the introduction of carboxylic groups at the CNT surface could trigger unattended and detrimental cellular responses [11]. Such parameters must therefore be thoroughly controlled and characterised to design safe and biocompatible nanotubes applicable as delivery systems. The post-synthesis surface modification of nanotubes with hydrophilic molecules, named functionalisation, has been reported as an efficient approach to enhance their water dispersibility and reduce their toxicity [12,13]. This can be performed by covalently attaching moieties at the surface of CNTs or by non-covalent interactions between nanotube surface and hydrophobic/aromatic regions of amphiphilic molecules [14].

To tailor nanotube function, therapeutic molecules or imaging probes can be added to functionalised CNT (*f*-CNT) side-walls [4]. By taking advantage of their inner cavity, *f*-CNTs can also be filled to keep the surface available for further modifications [15]. Contrast agents can be combined to nanotubes to generate CNT-based hybrids with clinical imaging capabilities [16]. If such hybrids display desirable targeting capabilities, they become versatile imaging tools for diagnostic applications [17,18]. CNT hybrids can also help tracking administrated nanocarriers to assess in real-time their spatial distribution and therefore measure their biodistribution profile [19]. The major medical imaging techniques, namely ultrasound, nuclear and magnetic resonance imaging (MRI), display limitation in terms of sensitivity or image resolution. To improve this, the combination of synergistic imaging modalities in a single carrier, such as CNTs, could be particularly valuable [20]. Beyond the promising properties of CNT-based hybrids for multi-imaging capabilities, their dimensions need to be optimised in order to control their intrinsic imaging properties, improve their accumulation in target cells and enhance their biocompatibility profile. This dimension refinement is essential to demonstrate the potential of CNT-based hybrids and confirm their safety before conducting clinical studies.

A wide range of studies have also reported on the development of carbon nanotubes for brain delivery, with results showing that adequate functionalisation is essential to produce biocompatible CNTs capable of local or systemic delivery of therapeutics to brain cells [21].

In this review, a description of the physico-chemical properties and surface modification of CNTs needed for delivery will be presented. Moreover, the interaction between CNTs and mammalian cells will then be described, followed by a summary of their toxicity. Finally, we will look into the most recent advances involving CNT-mediated systemic brain delivery and *in situ* CNT biodegradation.

2. Physico-chemical properties and surface modification of CNTs for biomedical applications

2.1. Synthesis, classification and properties

Carbon nanotubes can be generated by electric arc discharge and laser ablation using vaporisation of graphite target [22,23]. Alternatively, they are synthesised by chemical vapour deposition which rely on the passage of carbon-containing vapours in a furnace containing metal catalysts [24]. CNTs can be classified as single-walled (SWNT) or multi-walled (MWNT) nanotubes, in accordance with the number of layers that compose a single nanotube (Fig. 1).

SWNT and MWNT exhibit a diameter of 0.4–2 nm and 10–100 nm, respectively [26]. Both types are utilised as delivery systems and display large aspect ratios with lengths ranging from 50 nm to several microns. The length and diameter can be tuned by controlling the production conditions, but the design of CNT-based delivery systems requires further post-synthesis shortening procedures to increase their biocompatibility and bioavailability [10,19]. A reduction in the CNT length to diameter ratio can be achieved by strong acid treatment, ultrasonication, steam-purification and mechanical methods [27–29].

The unique physicochemical properties of CNTs, namely high surface area and length-to-diameter ratio, optimal electrical conductivity, and thermo-chemical stability, make them particularly attractive for biomedical applications [30]. However, pristine CNTs must be functionalised to improve their hydrophilicity and biocompatibility.

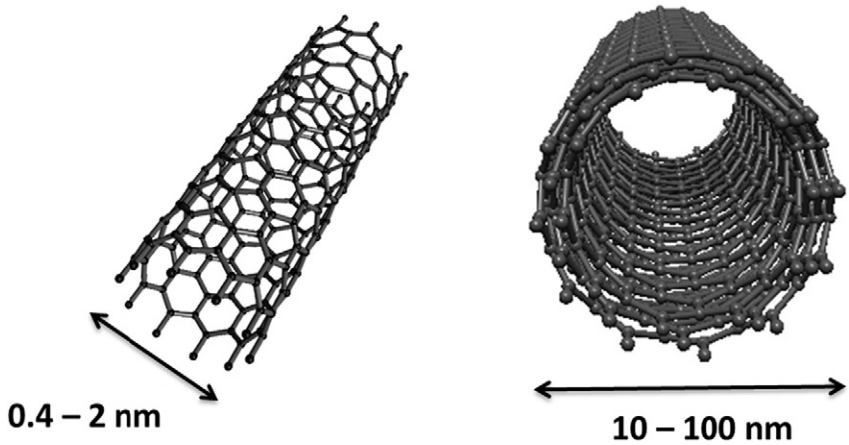

Fig. 1. Schematic representation of single-walled (SWNT) and multi-walled (MWNT) CNTs. Single and multi-walled CNTs have similar structures but different diameters. The figure was redrawn and modified from [25] and [26].

2.2. Non-covalent functionalisation

The delocalised aromatic system of nanotube layers makes them aggregate in bundles and results in their poor dispersibility in physiological aqueous environment [31]. The large surface area of CNTs enables non-covalent or covalent conjugation of hydrophilic molecules to enhance their dispersibility [13]. The non-covalent modification consists in the physical adsorption of amphiphilic surfactant molecules onto the surface of the CNTs by Van der Waals interaction, π-π stacking or electrostatic interaction [32–34]. The main advantages of this approach are the preservation of the intrinsic optical properties of CNTs and the simplicity of the functionalisation procedure [30]. However, the interaction after coating should be limitedly affected by the presence of salt to maintain the stability of the complex in a physiological environment. Biocompatible polymers (*e.g.* Pluronic® F-127, polyethylene glycol (PEG)) [35,36], gum arabic [37], single-stranded DNA (ssDNA) [38] and proteins (*e.g.* bovine serum albumin, BSA) [39,40] were reported to increase the dispersibility of CNTs.

2.3. Covalent functionalisation

Covalent CNT functionalisation relies on the chemical bonding of functional groups to the wall of CNTs, and is also referred as chemical functionalisation [41]. In contrast to the non-covalent approach, chemical functionalisation leads to strong and stable chemical bonds grafted onto the sp^2 carbon framework of the tips and sidewall of CNTs [42]. The functionalisation of CNT can be carried out by oxidation under strong acidic conditions, which produces carboxylic acid groups and shortening of CNTs [43]. However, the introduction of carboxylic groups at the surface of CNTs has been associated with cellular toxicity [28,44]. Further reactions can conjugate carboxylic acid groups to an amine or alcohol groups to obtain amide or ester linkage, respectively [13]. In addition to oxidation, another common chemical reaction is the 1,3-dipolar cyclo-addition using the condensation of an amino acid and an aldehyde [45].

Both covalent and non-covalent functionalisations have shown their ability to increase the dispersibility of nanotubes in a physiological environment, making them available to cross cell membranes and accumulate into intracellular compartments.

3. Uptake and cellular fate of functionalised CNTs (*f*-CNTs) in cancer cells and macrophages

Efficient uptake properties of CNTs have encouraged their use as drug delivery systems. After crossing the plasma membrane, the intracellular pathways of CNTs can lead to organelle accumulation and/or nanotube elimination [46–50]. The characterisation of their mechanisms of uptake and elimination remains of great interest to shape the delivery properties of CNTs and ensure their bioclearance.

3.1. Passive versus active mechanism

A leading study by Pantarroto and collaborators demonstrated that the high aspect ratio of CNTs allowed them to efficiently cross cellular membranes [9]. Subsequently, a dual mechanism of uptake into mammalian cells has been described [51]: CNTs were shown to use either an endocytic pathway or the passive diffusion to penetrate through cellular membranes (Fig. 2). In the endocytic mechanism, CNTs are internalised inside vesicles, named endosomes, before being directed to the lysosomes localised in the perinuclear compartment [52]. The energy-dependent uptake of nanotubes was described as predominantly clathrin-dependent for both SWNT and MWNT [53,54]. Kang and colleagues showed that SWNT/doxorubicin complexes, conjugated *via* hydrophobic π stacking, were internalised using the endocytic pathway and accumulated into the perinuclear lysosomal compartment of endothelial progenitor cells [49]. While SWNT remained entrapped into lysosomes, DOX detached in the acidic lysosomal environment due to the pH-dependent π-π stacking interaction, diffused into the cytoplasm and reached the nuclear compartment to induce cell killing.

In contrast, the passive diffusion of CNTs, also called needle-like penetration, results in the simple diffusion of CNTs through the cellular membrane without need of energy consumption [9,55]. Following computational and electron microscopy studies, the passive diffusion of *f*-CNTs through the phospholipid bilayer membrane, has been broken down in three steps: i) landing and floating of the *f*-CNTs on the membrane surface; ii) penetration of the lipid head groups; and iii) sliding through the lipid tails (Fig. 2) [56,57].

A model explaining the differential mechanism of uptake between active and passive mechanisms has been proposed by Yan and coworkers [51]. Accordingly, CNT clusters would be internalised by an endocytic mechanism, whereas individualised nanotubes would enter the cell by membrane diffusion (Fig. 2).

Interestingly, despite the significant effort dedicated to the characterisation of CNT internalisation pathways, there is no report suggesting that passive transport is preferred to endocytosis for drug delivery applications. However, one could indicate that both pathways support the versatile capabilities of CNTs to cross biological membranes.

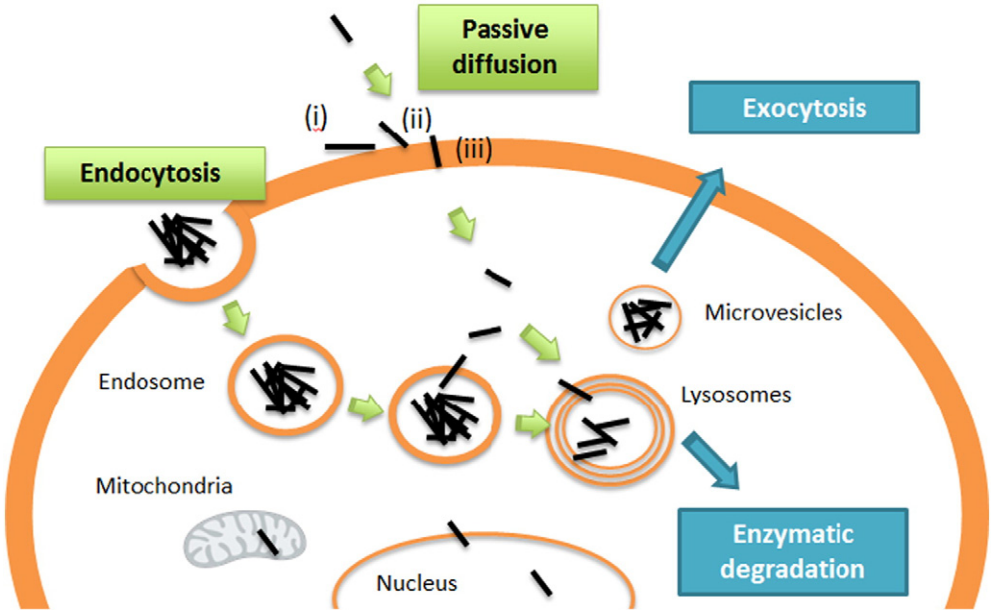

Fig. 2. Uptake and cellular fate of *f*-CNTs in mammalian cells. The bundled MWNTs bind to cellular membranes and are then internalised into cells by endocytosis. In the endosomes, bundles release single MWNT, which penetrate through endosomal membranes and enter the cytosol. Alternatively, short and individualised CNTs (i) land on the surface of the plasma membrane, (ii) penetrate the lipid head groups and finally (iii) slide through the lipid tails to passively diffuse through the cell membrane. Both residual bundled MWNT in endosomes and free MWNT in the cytosol are recruited into lysosomes. CNTs can be excreted by exocytosis (not shown) or in autophagic microvesicles in case of cellular stress. Another exit mechanism has been reported in polynuclear neutrophils and macrophages where nanotubes are digested enzymatically. CNTs are also able to enter organelles and the nucleus. The figure was redrawn and modified from [51].

3.2. Differential uptake between non-phagocytic and phagocytic cells

The use of CNTs for drug delivery entails their capture by macrophages, which participate in homeostasis and physiological defence mechanisms [58–60]. These cells are especially involved in the removal of external materials by phagocytosis, a cell endocytic pathway similar to endocytosis but involving the uptake of large particles (~1 μm). Both endocytosis and phagocytosis are energy-dependent mechanisms that are impeded at low temperature [53]. Phagocytic cells take up CNTs mainly through phagocytosis but the blockade of this energy-dependent pathway still allows the uptake of CNTs by passive diffusion [61]. SWNTs coated with phospholipid-polyethylene glycol (PL-PEG) were found to cross the cell membrane of non-phagocytic cells (ASTC-a-1, COS7, MCF7, EVC304) by passive diffusion and accumulate into mitochondria, whereas in macrophages (RAW264.7), CNTs accumulated in lysosomes following a phagocytic mechanism [62]. These results suggest that the internalisation mechanism of nanotubes was dependent not only on the properties of CNTs but also on the phagocytic nature of cells. Within the same population of phagocytic cells (human monocyte-derived macrophages), a study intended to establish a differential uptake of fluorescently labelled nanotubes as function of their length [63]. Constructs above 400 nm in length were mainly localised in endocytic vesicular structures, while the fluorescent signal from shorter CNTs was more diffuse, supporting their extra-vesicular localisation in cell cytoplasm.

Overall, these results suggest that shortening of CNTs enhances their passive diffusion uptake mechanism, even in phagocytic cells.

3.3. Cellular fate of CNTs

Following their passage through cellular membranes, CNTs were reported to accumulate in various subcellular compartments, such as the cell cytosol [61], endosomes [54,64], the perinuclear region [65], mitochondria [62,66] or the nucleus [51], according to their physicochemical properties and functionalisation. Exocytosis and biodegradation of CNTs have also been reported as possible cell elimination mechanisms for this material [46,47,50]. The description of such outcomes is crucial to confirm the potential of CNT bio-elimination, ultimately lowering the risk of CNT toxicity.

3.3.1. Exocytosis

Taking advantage of the intrinsic CNT photoluminescence properties, SWNTs were tracked by Jin and colleagues in real-time using single particle tracking, and showed similar endocytosis and exocytosis rate (Fig. 2). [46,47]. Using Raman spectroscopy mapping, Neves and colleagues found that oxidised and RNA-wrapped double-walled CNTs (DWNTs) accumulated in cells over 3 h before being progressively released out of the cells over a 24 h period [67]. It recently emerged that the process of exocytosis could also be induced under stress conditions. Naive human monocyte macrophages and endothelial cells exposed to stress were able to release microvesicles containing CNTs [68]. This mechanism could eliminate exogenous and toxic carbon material by inducing the formation of autophagic microvesicles [69].

3.3.2. Enzymatic degradation

The enzyme degradation of CNTs was reported as a possible mechanism by which cells eliminate this material (Fig. 2). Studies by Allen and collaborators provided evidence of the degradation of oxidised SWNTs through enzymatic catalysis in abiotic conditions [70, 71]. Following the incubation of carboxylated SWNT with horseradish peroxidase in low H_2O_2 concentrations (40–80 μM), a combination of techniques including transmission electron microscopy (TEM), Raman and ultraviolet-visible-near-infrared (UV-NIR) spectroscopy, and showed that digested CNTs displayed reduced absorbance, dramatic length shortening and disappearance of their discriminating G- and D-bands. It was later proposed that the presence of carboxylic group and defects at the surface of CNTs are a prerequisite to trigger the interaction with the oxidative agent and that nanotube degradation was function of the defect density [72]. Using similar techniques, it was demonstrated that *in vitro* exposure of SWNTs to neutrophils followed by enzymatic digestion with myeloperoxidase (MPO) promoted alterations in CNT structure [73,74]. These findings were supported by *in vivo* studies using TEM, Raman spectroscopy and photoacoustic imaging, which

showed degradation of SWNTs in lung tissue following pharyngeal administration in mice [48,75]. Using TEM and Raman spectroscopy, our group also found evidence of SWNT degradation in mouse brain after stereotactic injection [76]. In a recent study, the amount of CO_2 released from the enzymatic digestion of nanotubes in contact with horseradish peroxidase was measured, with a CNT degradation rate of ~0.002% per day being reported, which corresponds to a half-life of ~80 years [77].

While studies confirm that CNTs can be enzymatically degraded, the notion of degradation is still broadly employed and future reports must provide qualitative and quantitative data regarding the formation of by-products induced by CNT enzymatic degradation, especially for *in vivo* investigations.

4. Biocompatibility of CNTs

The toxicity of CNTs has been widely reported and is of major concern for human use [78]. It is accepted that CNTs are heterogeneous material with certain physico-chemical properties that can promote deleterious biological responses [11]. Therefore, the use of CNTs, applied to the drug delivery field, requires the design of materials with enhanced biocompatibility properties to ensure the safe translation of this material into clinical use.

4.1. Main properties of CNTs influencing toxicity

CNTs exhibit heterogeneous purity, length, type of functionalisation and surface interaction with plasma proteins that can affect their cellular toxicity. CNT toxicity mechanisms have been mostly explored by measuring cell viability, cell inflammation and the production of reactive oxygen species (ROS).

The concept of cellular toxicity can be described using the Hierarchical Oxidative Stress Model associating the cell toxicity mechanisms with the intracellular levels of ROS [79] (Fig. 3). At low concentrations, ROS can be neutralised by anti-oxidants - *e.g.* glutathione (GSH), and detoxification enzymes. When the antioxidant defence is overwhelmed, further damages occur such as lipid peroxidation, change in cell morphology and genotoxicity [80,81]. Excessive ROS production initiates an inflammatory response through the release of cytokines and chemokines [80,82]. Finally, further ROS production induces the release of apoptotic factors leading to cell death [83]. The measurement of such end points relies more frequently on the quantification of cell metabolism, DNA content, membrane disruption or cellular apoptosis induction [28,84].

In vitro toxicity studies comparing physico-chemical properties of CNTs are summarised and classified in Table 1.

The main factors involved in CNT toxicity are reported hereafter.

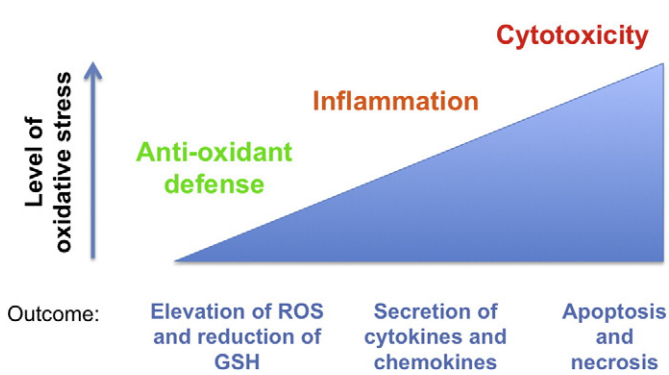

Fig. 3. Hierarchical Oxidative Stress Model. This model associates the cell toxicity mechanisms with the intracellular levels of ROS. The figure was re-drawn and modified from [85].

4.1.1. Impurities

Catalyst remnants from the CNT synthesis, such as nickel (Ni), cobalt (Co), iron (Fe) and molybdenum (Mo), and amorphous carbon, localised at the surface of nanotubes or entrapped within the CNTs, can lead to oxidative stress, anti-oxidant depletion and a reduction in cell viability [86,101,102]. Several methods can be used to reduce the presence of impurities including high-temperature annealing, acidic treatment by reflux or steam-purification [101,103,104]. It has been demonstrated that CNTs free of catalyst metals and graphitic contaminants are unlikely to result in any inflammatory response or impairment of phagocytosis [105].

4.1.2. Dimensions

CNT length has been shown to greatly influence CNT toxicity. Extremely long CNTs (10–20 μm) displayed asbestos-like behaviour and long bioretention in peritoneal mesothelium [11]. When macrophages attempted to engulf long CNTs displaying larger dimension than the actual cell, it resulted in frustrated phagocytosis leading to formation of granuloma [106]. Such lengths are impractical for drug delivery and the shortening of CNTs has emerged as a logical requirement for biomedical applications. Following the same mechanism, MWNT of 2.4–10 μm length, coated with Pluronic® F-127, exerted higher toxicity than shorter materials (0.4–1.4 μm) in a murine macrophage cell line, while shorter CNTs led to higher inflammatory response [93]. This opposite effect of CNT length on cell viability and inflammation suggested that the Hierarchical Oxidative Stress Model could not always be applied to characterise the toxicity of CNTs. Other studies reported disparities between the impact of CNTs on cell viability and inflammation/oxidative responses [97,101,107,108]. The effect of nanotube diameter on cellular toxicity was described only in few studies and contradictory results were reported, thus limiting any statement about the influence of such parameter [109,110].

4.1.3. Defects

Defects at the surface of nanotubes may be topological (*e.g.* ring shapes other than hexagon), sp^3 hybridised carbon atoms, incomplete bonding defects, doping with elements other than carbon, as well as various functionalities at the surface [111]. Studies by Fenoglio and Muller established that the presence of defects at the surface of CNTs triggered acute pulmonary toxicity and genotoxicity [84,112]. It was later reported that the shortening of CNTs by sample ultra-sonication using concentrated acid solution produced defects at the surface of the nanotubes, which were correlated with enhanced pro-inflammatory and pro-oxidative response [28]. Such report demonstrated that the shortening process could be associated with the formation of defects leading to inflammation and cytotoxicity.

Due to the heterogeneity of CNTs and the lack of data about CNT surface characterisation, the association between CNT toxicity and their physico-chemical properties can be puzzling. For example, Cheng and collaborators found that short MWNT (0.2 ± 0.1 μm) altered the development of zebrafish embryo, while long MWNT (0.8 ± 0.5 μm) showed reduced embryo-toxicity [113]. Although the authors concluded that nanotube length influenced the toxicity on embryos, the formation of defects at the surface of nanotubes induced by prolonged ultra-sonication in concentrated acid could just as well be responsible for the toxicity measured [113].

4.1.4. Functionalisation

Efficient dispersion resulting in individualised CNTs must be achieved for drug delivery applications in order to reduce the formation of CNT aggregates and increase their biodisponibility [19]. The type and degree of functionalisation tend to influence CNT toxicity. Surface functionalisation of nanotubes with carboxylic groups, using acid treatment, showed increased defect formation at the surface of CNTs adsorbing catalyst particles and generating free radicals [114]. Human neuroblastoma cells exposed to different concentrations of oxidised MWNT showed

Table 1
In vitro comparative studies of *f*-CNTs toxicity.
List of abbreviations in this table: AM: alveolar macrophages; ATII: primary human alveolar type-II epithelial cells; ATP: adenosine triphosphate; BAL: bronchus-alveolar lavage fluid; BCA: bicinchoninic acid assay; CHO: Chinese hamster ovary cells; CXCL-2: chemokine CX motif ligand 2; DPPC: dipalmitoylphosphatidylcholine; EthD-1: ethidium homodimer-1; gCNTs: grounded carbon nanotubes; GSH: glutathione; hprt: hypoxanthine-guanine phosphoribosyltransferase; LDH: lactate dehydrogenase; MTS: 3-(4,5-dimethylthiazol-2-yl)-5-(3-carboxymethoxyphenyl)-2-(4-sulfophenyl)-2H-tetrazolium; MTT: 3-(4,5-Dimethylthiazol-2-Yl)-2,5-Diphenyltetrazolium Bromide; NLRP3: nucleotide-binding domain leucine-rich repeat and pyrin domain containing receptor 3; NO: nitric oxide; NT1: uncoated carbon nanotubes; NT2: carbon nanotubes coated with acid based polymer; NT3: carbon nanotubes coated with polystyrene-based polymer; RNS: reactive nitrogen species; SWNT-PEG: single-walled carbon nanotubes functionalised with polyethylene glycol; TUNEL: terminal deoxynucleotidyl transferase dUTP nick end labelling; TT1: human alveolar type-I-like epithelial cells; XTT: 2,3-bis-(2-methoxy-4-nitro-5-sulfophenyl)-2H-tetrazolium-5-carboxanilide; WST-1: 4-[3-(4-iodophenyl)-2-(4-nitrophenyl)-2H-5-tetrazolio]-1,3-benzene disulfonate; ↗: increase; ↘: decrease.

	CNT type and properties	Functionalisation	Cell model	Viability/proliferation/morphology	ROS/inflammation/genotoxicity	Reference
Catalyst impurities	SWNT (Fe: 0.23 *vs* 26 wt.%)	Serum coated	Mouse macrophages (RAW 264.7)	—	26 wt.% Fe: ↗ NO; ↗ superoxide radicals; ↗ GSH content	[86]
	MWNT (Fe: 4.2 *vs* 12.0 wt.%)	Pluronic® F-108 coated	Rat pheochromocytoma (PC12) cells	12.0 wt.% Fe: ↘ cell viability (CCK-8 assay), ↗ cytoskeleton disruption, ↘ neurite outgrowth	12.0 wt.% Fe: slight ↗ of intracellular ROS	[87]
	MWNT (Fe: 0.05 *vs* 0.5 wt.%)	Serum coated	Murine alveolar macrophages (MH-S)	0.5 wt.% Fe: ↗ of LDH release	0.5 wt.% Fe: ↘ GST; ↗ lipid peroxidation	[88]
	MWNT (Ni: 2.54–5.47 wt.%)	Serum coated	Primary alveolar macrophages	Ni-rich CNTs: ↘ cell viability (MTS assay)	Ni-rich nanotubes: ↗ pro-inflammatory cytokines (IL-1β & IL-18); ↗ NLRP3 activation	[89]
	MWNT (Fe: 0.08 *vs* 4.24 wt.%)	Gum arabic-coated	Human alveolar epithelial cells (A549)	No significant difference on cell viability (LDH, MTT and XTT assays)	—	[90]
CNT length	SWNT (length: 0.5–2 μm *vs* 5–30 μm)	Polyvinylpyrrolidone coated	Dynamic cell culture system of human alveolar epithelial cells (A549)	Long CNTs: ↘ cell proliferation (BCA assay)	Long CNTs: ↗ pro-inflammatory cytokines (IL-8); ↗ ROS production	[91]
	MWNT (average length: 0.6 μm *vs* 3 μm *vs* 20 μm)	Serum coated	Human alveolar type-I-like epithelial cells (TT1) Primary human alveolar type-II epithelial cells (ATII) Alveolar macrophages (AM)	Long CNTs: ↗ cell viability (MTT and LDH assay) in epithelial cells (TT1, ATII) and ↘ cell viability in AM	Long CNTs: ↗ pro-inflammatory response (IL-6, IL-8 and MCP-1) in epithelial cells (TT1, ATII) but ↘ pro-inflammatory effect in AM	[92]
	MWNT (length: 0.4–1.4 μm *vs* 2.4–10 μm)	Pluronic® F-127 coated	Murine macrophages (RAW264.7) Human breast cancer cells (MCF-7)	Long CNTs: ↘ cell viability (CellTiter-Blue assay and trypan blue counting)	Long CNTs: ↘ pro-inflammatory response (TNF-α and IL-12); ↗ ROS production	[93]
	MWNT (average length: 150 nm *vs* 20 μm)	Dispersion in DPPC solution	Salmonella typhimurium *Escherichia coli* Chinese hamster ovary cells (CHO)	—	Both CNT lengths did not affect genotoxicity (Ames test, *in vitro* chromosome aberration assay)	[94]
	SWNT (length: 400–800 nm *vs* 1–3 μm *vs* 5–30 μm)	Serum coated	Human bronchial epithelial cells (BEAS-2B) Human lymphoblastoid B cells (MCL-5)	CNTs with middle-range length (1–3 μm) ↘ cell viability (cytokinesis-blocked micronucleus assay)	CNTs with middle-range length (1–3 μm) ↗ hprt forward mutation assay and ↗ ROS production	[95]
	MWNT (average length: 950 nm *vs* 250 nm)	Carboxylation *vs* amination	Whole human blood	Long aminated CNTs: ↘ platelet viability (CD61 labelling)	—	[96]
Presence of defects	MWNT Grounded CNTs (gCNT) with structural defects *vs* heated CNTs with few oxygen functionalities	Oxygen functionalities introduced by grinding	Cells from broncho-alveolar lavage fluid (BAL)	gCNTs ↘ cell viability (LDH and protein content, macrophages and neutrophils counting in BAL)	gCNTs ↗ pro-inflammatory response (IL1-β, TNF-α) gCNTs ↗ genotoxicity (↗ micronucleated binucleated cells)	[84]
	MWNT CNTs of 9.5 μm *vs* shortened CNTs of 4.8 μm with high content of structural defects	Short CNTs: oxygen functionalities introduced by acid treatment and ultra-sonication	Mouse macrophages (RAW 264.7)	No difference between short and long CNTs in terms of cell viability (WST-1)	Short CNTs: ↗ pro-inflammatory response (TNF-α and CXCL-2) and ↗ pro-oxidative response	[28]

(continued on next page)

Table 1 (*continued*)

	CNT type and properties	Functionalisation	Cell model	Viability/proliferation/morphology	ROS/inflammation/genotoxicity	Reference
CNT functionalisation	MWNT Uncoated CNTs (NT1) *vs* CNTs coated with acid based polymer (NT2) or polystyrene-based polymer (NT3)	Polymer coated	Mouse macrophages (RAW 264.7)	Cell viability (MTT) was higher in NT1 > NT2 > NT3	Inflammation (CXCL-2) and oxidative stress (HO-1) were higher in NT3 > NT2 > NT1	[97]
	MWNT Pristine CNTs *vs* oxidised CNTs *vs* amino functionalised CNTs	Oxidised CNTs or amino-functionalised CNTs with ethylene-diamine	Mouse macrophages (RAW 264.7)	All CNTs ↘ proliferation (intracellular ATP) and viability (extracellular ATP). Oxidised CNTs ↗ *anti*-proliferative effect	–	[44]
	MWNT Oxidised CNTs at increased density	Oxidation of CNTs for 1 to 8 h in acid	Mouse macrophages (RAW264.7)	Increased density of carboxylic groups ↗ cell death (MTT) and ↗ cell apoptosis (TUNEL) in a concentration manner	High density of carboxylic groups: ↗ RNS in a concentration manner	[98]
	SWNT Covalent functionalised CNTs *vs* non-covalently functionalised CNTs	SWNT-phenyl-SO3Na (increased density ratio) *vs* Pluronic® F-108 coated SWNT	Human dermal fibroblasts	Pluronic® coated CNTs: ↗ cytotoxicity (calcein AM & EthD-1, MTT); SWNTs degree of functionalization ↘ cytotoxicity	—	[99]
	SWNT Pristine SWNT *vs* SWNTs functionalized with polyethylene glycol (SWNT-PEG)	Pristine SWNT *vs* SWNT-PEG	Neuronal PC12 cells	SWNT-PEG: ↘ cytotoxicity (MTT, XTT, LDH); pristine SWNTs induced spindle shape morphology and SWNT-PEG inhibited dendrite growth	Compared to pristine SWNTs, SWNT-PEG ↘ ROS generation and ↗ GSH level; SWNT-PEG ↘ gene expression associated to cytotoxicity	[100]
	MWNT Amidated CNTs *vs* aminated CNTs	Oxidation + amidation *vs* 1,3-dipolar cycloaddition reaction	Peritoneal macrophages Lymphocytes B & T	Both CNT types did not affect cell viability	Amidated CNTs ↗ inflammation (IL-6, TNF-α) & ↘ LPS restimulation (IL-6, TNF-α)	[12]

dose-dependent decrease in cell viability [114]. In contrast, T-lymphocytes incubated with CNTs functionalised by 1,3-dipolar cycloaddition — forming aminated nanotubes — did not increase the apoptotic proportion of immune cells and preserved their inflammatory functionality by maintaining their interleukin secretion following the activation by lipopolysaccharides (LPS) [12].

4.1.5. Protein binding

Protein binding to the surface of nanotubes occurs in a physiological environment, such as the blood circulation system, but can also be used as a strategy for CNT dispersion. The compact and multi-layer form of bovine fibrinogen (BFG) proteins was shown to reduce the toxicity of CNTs proportionally to the degree of adsorption onto the surface of nanotubes [115]. In contrast, Dutta and colleagues showed that MWNT dispersed in serum bovine albumin induced pulmonary fibrosis [116]. By coating the same material with Pluronic® F-108, the amphiphilic polymer was able to protect the lysosomal membrane from CNT damage and abolish the formation of pulmonary fibrosis [116].

4.2. Influence of cell model on CNT toxicity

Recent studies have highlighted that the toxicity of nanotubes is dependent not only on their physico-chemical properties but also on the cellular model used for toxicity assessment. In a study by Foldbjerg and colleagues, epithelial cancer cells (A549), human monocyte-derived macrophages (THP-1) and mouse macrophages (J774) were exposed to SWNT dispersed in BSA. Incubation at 10 μg/ml led to reduction in cell viability, necrosis, reduction of phagocytic ability, increased ROS levels and cytokine release in J774 cells, while A549 and THP-1 cells treated in the same conditions were not affected [117]. As J774 cells exhibited the highest phagocytic properties, the authors suggested that the toxicity of SWNT was mostly dependent on the uptake capacities of the cellular model used. However, the lack of inclusion of primary cells in this study could raise interrogations about the pertinence of such results *in vivo*. In a similar study, the toxicity profile of pristine MWNT of different lengths (0.6, 3 and 20 μm) was assessed in primary lung epithelial cells (TT1), primary human alveolar type-II epithelial cells (ATII) and primary lung alveolar macrophages (AM) [92]. Long MWNT led to an increase in lactate dehydrogenase (LDH) release, cell viability and cytokine secretion in AM cells, while shorter MWNT induced a stronger response in epithelial cells. In an interesting study by Asghar and colleagues, which focused on the toxicity of CNTs towards germline cells, no significant toxicity was found upon exposure of human sperm samples to 1–25 μg/ml of carboxylated SWNTs, although higher concentrations resulted in a significant increase in the production of reactive superoxide species [118].

The different response of epithelial and macrophage-like primary cells to CNTs highlights the need to select appropriate and relevant models to test *in vitro* the toxicity of CNTs. In our opinion, epithelial cells, macrophages and cells from the reticuloendothelial system should be included in any studies aimed at assessing toxicity of CNT-based nanocarriers.

4.3. Mechanisms of cellular toxicity triggered by CNTs

The mechanisms of cellular toxicity induced by nanotubes have been essentially described using pristine CNTs and were mostly related to the production of oxygen radicals [50] (Fig. 4).

The induction of oxidative stress activates signalling pathways mediating inflammation and, ultimately, to cellular toxicity. Activation of NF-κB or AP-1 transcription factors by CNTs has been directly involved in upregulating genes involved for the release of cytokines such as IL-1, IL-6 and TNF-α [50,119]. CNT-related oxidative stress could result in oxidation of mitochondrial phospholipids and nicotinamide adenine dinucleotide phosphate (NADPH) oxidation leading to inflammation and apoptosis, but also positive outcomes such as CNT biodegradation in neutrophils [71,120].

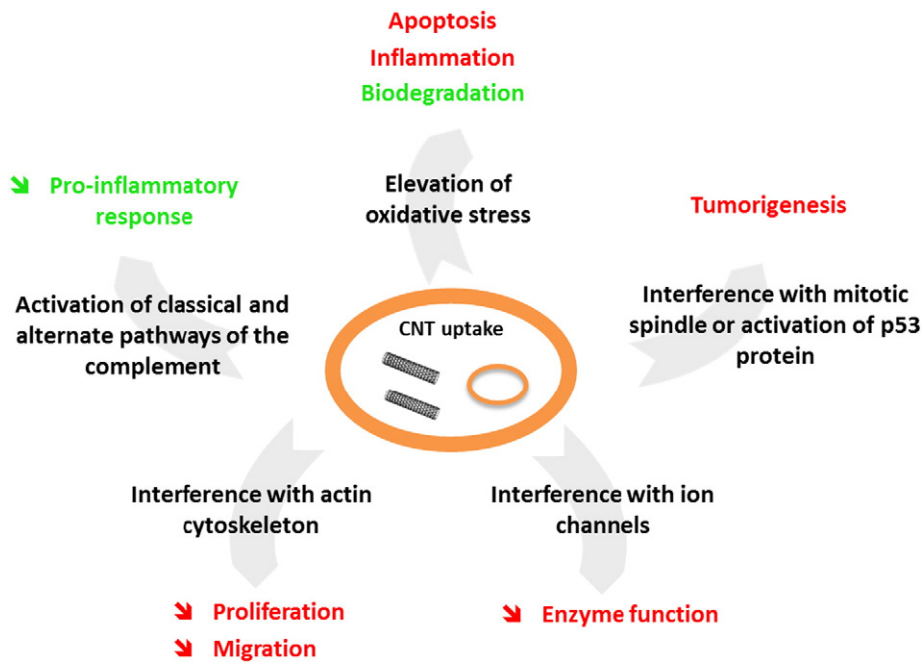

Fig. 4. Molecular mechanisms induced by CNT uptake. Schematic representation of the main molecular and cellular responses associated with CNT internalisation by cells. Cell exposure to CNTs could have negative effects, namely oxidative stress which can promote inflammation, mitochondrial oxidation and activation of apoptosis, blocking of ion channels leading to loss of enzyme function and cytoskeleton interference imparting proliferation and migration. Effects reported as positive include activation of the complement system which promotes phagocytosis and biodegradation of the CNTs.

Several non-oxidative stress-dependent effects were found related to the cellular accumulation of CNTs, such as the blocking of ion channels leading to loss of enzyme function, the interference with the cytoskeleton impacting proliferation, migration and phagocytosis, and the potential induction of a tumourigenic response [121–123]. It was reported that SWNT and DWNT could be responsible for activating the classical and alternate pathways of the complement system [124]. This was further associated with increased cellular infiltration and phagocytosis, as well as reduced pro-inflammatory cytokine secretion, thus supporting the beneficial effect of complement activation triggered by CNTs [125].

4.4. In vivo toxicity studies in non-brain tissues after intravenous administration of CNTs

A majority of pre-clinical toxicological studies assessed the toxicity of CNTs after pulmonary inhalation/exposure [10,106]. However, drug delivery mediated by CNT carriers requires the study of their toxicity following intravenous (i.v.) administration. In most reports, this evaluation was done using histological analysis [58,126,127], blood cell counting [128] and inflammation detection [126,127] in organs and blood. A summary of the studies reporting the toxicity of *f*-CNTs in murine models is presented in Table 2.

Dispersion was shown to be a key factor influencing CNT toxicological effect. Indeed, purified pristine MWNT injected intravenously accumulated mainly in the lungs as large aggregates, causing short-term respiratory distress [58]. The intravenous injection of pristine MWNT was also shown to form large CNT aggregates in liver and lungs and induce inflammatory cell infiltration around the airways and blood vessels in lung tissue [127]. In contrast, the i.v. injection of purified SWNT dispersed in 1.0% wt Tween®-80 in mice resulted in limited organ toxicity, despite large accumulation in liver, lung and spleen organs [133]. An increase in GSH level in liver and lungs suggested the induction of oxidative stress but the level of TNF-α in serum remained unchanged. In another study, SWNT covalently or non-covalently functionalised with PEG was injected i.v. in athymic mice. Histological and blood analysis of liver and spleen did not reveal any acute or chronic toxicity up to four months post administration [128], thus suggesting that attachment of appropriate functional groups at the surface of CNTs is a critical parameter to enhance their biocompatibility. More recently, toxicity of chemically functionalised MWNT to spleen was evaluated over 2 months, with no functional or histological modifications detected [126]. However, MWNTs were shown to transfer from the red pulp to the white pulp over time, suggesting the formation of a splenic adaptive response.

Overall, the induction of *in vivo* inflammatory responses by *f*-CNTs is reduced but the persistence of such materials in major organs (*i.e.* lungs, liver and spleen) still requires further toxicological investigation. Moreover, there is currently no consensus about what animal models should be used to assess the short and long-term impact of CNT exposure in biological tissues. It is important that clear guidelines are established by the scientific community, so that the results and their interpretation/comparison are not affected by the different testing methods. Nevertheless, the results available to date suggest that i.v. injection of properly functionalized CNTs is well-tolerated and their use as carriers for therapeutic and imaging applications can be justified.

5. CNTs as carriers for therapeutic brain delivery

The delivery of therapeutic molecules to the brain is severely restricted by the presence of the blood-brain barrier (BBB), a complex network comprising brain endothelial cells, astrocytes and other support cells, that control the influx and efflux of nutrients and other molecules to the brain parenchyma. For this reason, treatment of complex neurodegenerative disorders and brain gliomas remains a challenge. When particle size is not small enough to overcome the BBB size restriction (*i.e.* <100 nm), nanoparticle-based brain-targeted therapeutic approaches have, thus far, taken advantage of the existing physiological mechanisms of transport to improve brain delivery. Polymer- and lipid-based nanoparticles are usually decorated with targeting moieties to support receptor-mediated transcytosis across the BBB. The capacity of CNTs to cross the BBB by both receptor- or adsorptive-mediated

Table 2
Representative *in vivo* studies of *f*-MWNT and *f*-SWNT injected IV in murine models
List of abbreviations in this table: ALP: alkaline phosphatase; d: diameter; *f*-MWNT: functionalised MWNT; GPCRs: G protein-coupled receptors; inj.: injection; ISL: isoliquiritigenin; L: length; NS: non-significant; RES: reticulo-endothelial system; ↗: increase; ↘: decrease.

	CNT type & functionalisation	Length (L) and diameter (d)	Murine model administrated dose treatment duration	Biological measurements	Histological & microscopic observations	Reference
MWNTs	- Functionalised with taurine (*f*-MWNT)	L: 269 ± 160 nm d: 12.6 ± 3.2 nm	♀ Kunming mice Dose: 60–100 mg/kg Until 60 days post-inj.	No alteration of RES phagocytic activity and oxidative stress in the spleen over 2 months	Spleen accumulation over 60 days without histological damages Relocation of *f*-MWNTs from the red pulp to the white pulp splenic region	[126]
	- Non-dispersed (MWNT) - Dispersed in Tween-80 (T-MWNT)	L: 0.5–5 μm d: 40 nm	BALB/c mice Dose: 100 μg/mouse Until 28 days post-inj.	Similar hepatic and renal functions between MWNT and T-MWNT groups at day 28	MWNT: in liver and lung and ↗ inflammatory cell infiltration T-MWNT: in the liver only and cleared at day 28	[127]
	- Oxidised (s-MWNT) - PEGylated (PEG-MWNT) MWNTs	L: 125 ± 75 nm d: 20 nm	Kunming mice Dose: 100 μg/mouse Until 3 days post inj.	NS change in blood count and in hepatic and renal functions	No accumulation observed histologically. No evidence of inflammatory response	[129]
	- Oxidised (o-MWNT) - Dispersed in Tween-80 (T-MWNT)	L: 356 ± 185 nm d: 10–20 nm	Kunming mice Dose: 10 or 60 mg/kg Until 60 days post inj.	T-MWNT: induced oxidative stress Both MWNTs altered hepatic function and liver gene expression (*e.g.* GPCRs, CYP450)	Both MWNTs induced hepatic damages (T-MWNT > o-MWNT) at high dose	[130]
	- Non-shortened and non-functionalised	L: 15 ± 5 μm d: 25 ± 5 nm	♂ C57BL/6 mice Dose: 1 mg/kg Until 7 day post-inj.	MWNTs induced T-cell activation in the spleen	MWNT aggregated in the lungs with size ↘ over time	[131]
	- Pristine (pMWNT) - Amino-functionalised (NH3-MWNT) - DTPA functionalised (DTPA-MWNT)	L: 0.5–2 μm d: 20–30 nm	♀ BALB/c mice Dose: 200–400 μg/mouse Until 24 h post-inj.	All MWNTs: normal biological functions; NH3-MWNT ↘ total protein pMWNTs ↘ ALP level without clear physiological impact	All MWNTs: in the liver and spleen without histological abnormalities pMWNT: lung accumulation and induced dyspnea, hunched posture and piloerection persisting 24 h post-inj. at high dose	[58]
	- Pristine MWNTs (pMWNT) - Low-degree of oxidation (o-MWNT) - High-degree of oxidation (O-MWNT)	Pristine: L: 10 μm O-MWNT: L: 500 nm All MWNTs: d: 20–30 nm	♂ Swiss mice Dose: unknown Until 28 days post-inj.	pMWNT & o-MWNT: ↗ hepatotoxicity, ↗ inflammatory response and ↗ oxidative damage at 7 days all recovered at 28 days O-MWNT did not affect biological measurements	pMWNTs: induced lethargy post-inj. and inflammatory cell infiltration in the liver o-MWNTs and O-MWNT induced slight or no inflammation	[132]
SWNTs	- Dispersion in Tween® 80	Purified SWNT L: 2–3 μm d:10–30 nm	♂ CD-ICR mice Dose: 40 μg, 200 μg or 1.0 mg/mouse Until 3 months post-inj.	Dose dependent hepatic injury Dose dependent oxidative damage in lung and liver	Black aggregates in lung, liver and spleen. Dose dependent inflammatory cell infiltration in the lungs. No evidence of hepatic or splenic damages.	[133]
	- PEGylated and conjugated with isoliquiritigenin (ISL-PEG-SWNT)	Dimensions not given	Wistar rats Dose: 200 μg/rat Until 24 h post-inj.	–	Vacuole formation in kidney tubules and myocardiac cells indicating toxicity (could be associated with ISL only)	[134]
	- Resuspended in BSA (BSA-SWNT) - Oxidised (o-SWNT)	BSA-SWNT: L: 0.1–1 μm d: 0.8–1.2 nm o-SWNT: L: 0.5–2 μm d: 1–2 nm	Sprague-Dawley rats (244 ± 8 g) Dose: 0.5 mg/rat Until 2 weeks post-inj.	Normal steatosis/cirrhosis, fatty acid metabolism, oxidative stress or transport gene expression in the liver	All SWNTs found in the liver, spleen, and lung 1 day post-inj. SWNTs were cleared after 14 days.	[135]
	- Non-covalent functionalisation with PEGylated phospholipids (PL-PEG-SWNT)	SWNT L = 100 nm	BALB/c mice Dose: 100 μg/mouse Until 3 months post-inj.	Normal liver and kidney function	PL-PEG-SWNTs accumulated in liver and spleen. No abnormal histology observed in these tissues	[136]
	-Non-covalently PEGylated (PEG-SWNT) - Covalently functionalised (PEG-o-SWNT)	PEG-SWNT: L: 100–300 μm d: 1–5 nm PEG-o-SWNT: L: 50–200 nm d: 1–5 nm	Nude mice Dose: 0.1 μmol/mouse 12 weeks post-inj.	No significant alteration of red blood cell and neutrophil counts	Presence of brown pigment in liver macrophages and in the spleen No alteration of organ and cell morphology but SWNTs still found in tissues after 4 months	[128]

energy-dependent pathways (transcytosis) and passive energy-independent mechanisms (needle-like crossing) constitutes a major advantage compared to other nanocarriers. In addition to the intrinsic ability to cross biological membranes, CNTs possess high surface area, which enables the loading and delivery of high doses of drugs to the therapeutic site, as well as intrinsic optical and thermal properties, with potential multimodal real-time tracking and photo-thermal applications. Although CNTs display optimal characteristics for use as nanocarriers in brain delivery, the intrinsic barrier-crossing capacity constitutes a limitation, due to unspecific bioaccumulation, and therefore specific brain target is important to increase brain accumulation and reduce systemic side effects.

5.1. Intracranial administration of CNT-based therapeutics

Local administration of therapeutics could bypass the BBB restriction and allow effective therapeutic doses to be achieved in the diseased tissues. This approach could be relevant in certain brain disorders, such as tumours and stroke, in which initial surgical approach is often necessary. Scheme 1 highlights the main strategies involving local CNT-mediated therapeutic brain delivery.

The conjugation of immunostimulatory CpG oligonucleotides to SWNTs was shown by Zhao and collaborators to be beneficial for the treatment of glioma-bearing mice [137]. Increased uptake of SWNT-CpG by tumour-associated inflammatory cells was found after a single intracranial injection (compared to the free CpG), which resulted in a strong anti-tumoural response, decreased tumour size and an increase in median animal survival time [137].

Taking advantage of the capacity of CNTs to absorb NIR radiation and convert it to heat, Santos and colleagues used CNTs for photothermal-mediated brain tumour therapy. The authors showed that a combination of intratumoural SWNT injection and NIR exposure in athymic GBM-bearing mice not only suppressed tumour growth compared to SWNTs or NIR *per se*, but also inhibited tumour recurrence for up to 80 days [138]. The electrical properties of CNTs prompted several research groups to use these carriers as scaffold for stem-cell mediated neuronal repair. Studies by Moon and colleagues in rats with stroke-induced brain injury revealed that focal injection of neural progenitor cell (NPC)-impregnated CNTs improved rat behaviour and reduced infarct cyst volume and area [139]. Similarly, pre-injection of amine-functionalised SWNTs onto the right lateral ventricle was shown to reduce the infarction area and improve behavioural functions following focal ischemic injury in rats [140]. The authors showed that the neuroprotective effect was achieved by reducing apoptosis, inflammation and glia activation and proposed that, even without NPCs, the high surface energy of the positively-charged SWNTs provided a favourable environment for neuronal regeneration. In a very recent study by Xue and colleagues, intraventricularly-injected aggregated SWNTs (aSWNTs) were shown to reduce methamphetamine (METH) addiction symptoms in mice by causing oxidation of METH-enhanced extracellular dopamine, which induced inhibition of the rewarding and psychomotor-stimulating effects of METH [141].

A previous study from our group revealed that the local *f*-MWNT-mediated delivery of siRNAs targeting caspase-3 (siCas3) successfully prevented neuronal death in an endothelin-1 (ET-1) rat stroke model (Fig. 5) [142]. This was supported by observation of a decrease in apoptosis in the penumbra lesion (Fig. 5A–C) and a statistically significant improvement in the "skilled reaching" behaviour test (Fig. 5D) for *f*-CNT:siCas3 treated rats, compared to animals receiving complexes of non-specific siRNA (siNEG) and *f*-CNT (*f*-CNT:siNEG) or siCas3 alone.

While the intracranial delivery of drugs could be of clinical utility, its wide application is nevertheless limited by the invasiveness of the technique and patient compliance. The versatility of nanotubes and their unique mechanism of interaction with cells paved the way for researchers to explore the use of CNTs as carriers for systemic drug delivery to the brain.

5.2. Systemic administration of CNT-based therapeutics

The ability of CNTs to penetrate biological membranes without perturbing the membrane integrity prompted researchers to test CNTs as vehicles for systemic therapeutic delivery across the BBB. Early

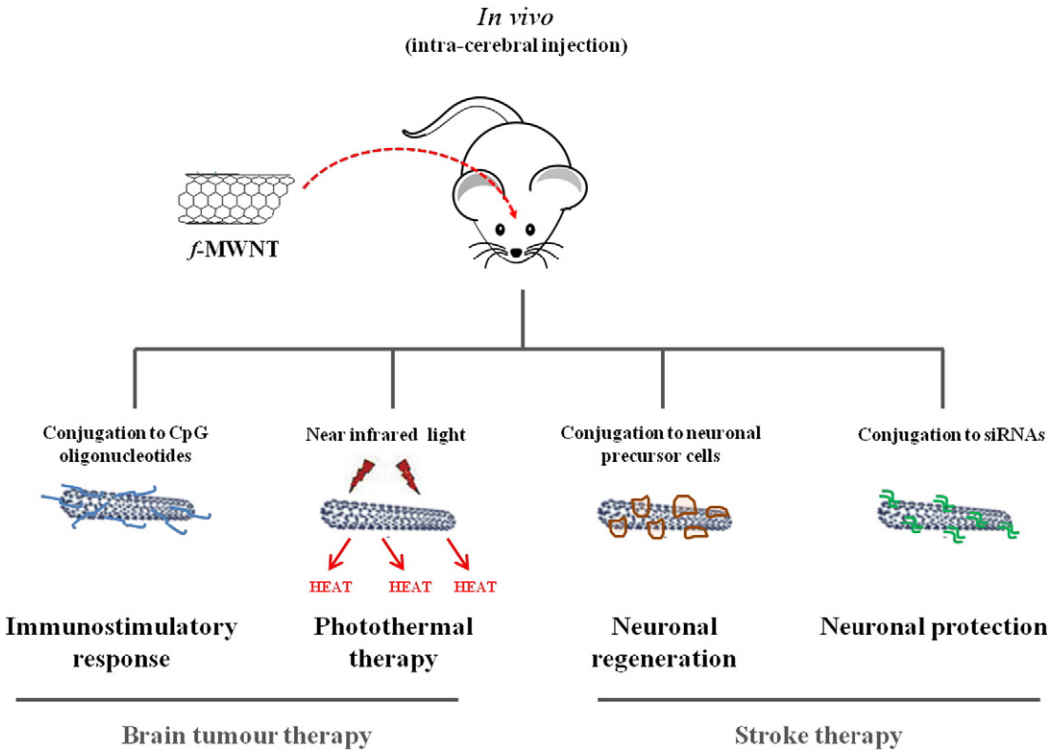

Scheme 1. Different stereotactically-delivered CNT-based strategies for brain therapy.

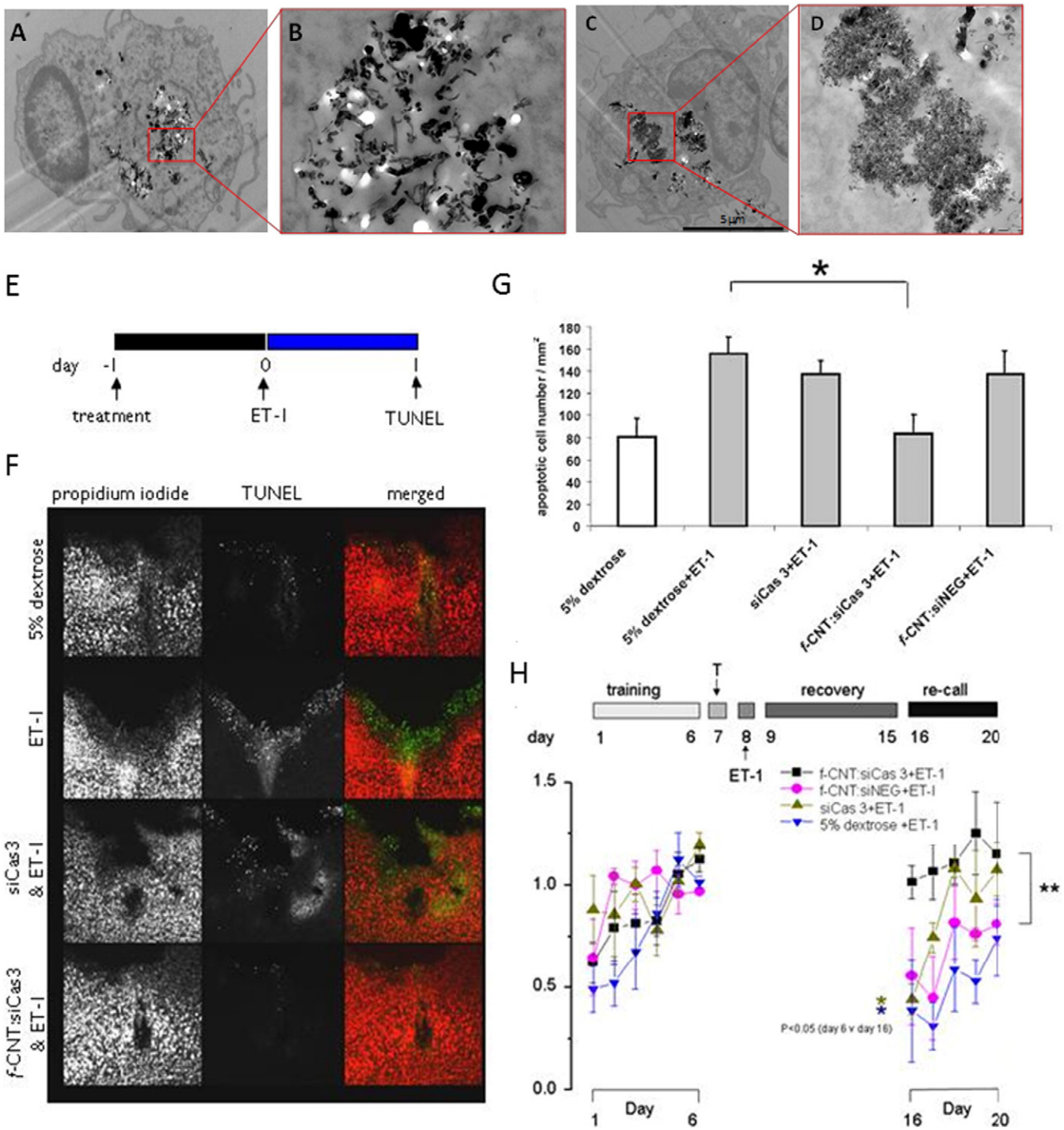

Fig. 5. *In vivo* uptake and degradation of *f*-MWNTs by microglia after intracranial administration into mouse brain. (A–D) TEM images of brain sections showing microglia cells engulfing MWNT-NH_3^+ within phagosomes 48 h after injection (red squares). (B, D) High magnification TEM images showing clear loss of tubular structure of MWNT-NH_3^+ in some phagosomes of the microglia (shown in D) even within 48 h post-administration (adapted from [76]). (E–H) RNAi using *f*-CNT *in vivo*. (E) Dosage regimen of the siRNA and endothelin (ET-1) into C57Bl/6 mice and (F) TUNEL staining of the mouse brain cortex after injection of 5% dextrose, *f*-CNT alone, siCaspase3 alone, and the siCaspase3:*f*-CNT complexes, followed by ET-1 injection. (G) The *f*-CNT:siCaspase3 group showed the least apoptosis quantitatively indicating effective and specific siRNA delivery *in vivo* compared to siRNA alone. (H) Behavioural analysis of rats after stroke induction in all the treated groups using the skilled reaching test (adapted from [142]).

evidence of efficient BBB translocation by CNTs was provided by studies in primary brain endothelial cells [143–145] and other commonly used *in vitro* BBB models [146].

5.2.1. In vitro BBB translocation

The interaction of *f*-MWNTs with the BBB has been previously investigated by our group using a BBB co-culture model comprised of primary porcine brain endothelial cells (PBEC) and primary rat astrocytes. This model replicates the physiological and biochemical features of the human BBB, including high trans-endothelial electric resistance (TEER), expression of membrane transporters and tight junction proteins [143]. TEM analysis revealed that *f*-MWNTs were quickly internalised (within 4 h) by PBEC cells *via* endocytosis, with *f*-MWNTs being released from endocytic vesicles near the abluminal side of

PBEC within 24–48 h (Fig. 6) [144]. Moreover, Scanning TEM (STEM) showed that this process did not cause any damage to the cell membrane (Fig. 6). Since no involvement of the tight junctions was detected during translocation, it was suggested that *f*-MWNTs use a transcellular route to cross the BBB.

In a subsequent study, the effect of CNT diameter on BBB translocation was investigated. Gamma counting was used to quantify the rate of translocation of "wide" (~35.9 nm diameter) (*w*-MWNTs) or "thin" (~9.2 nm) (*t*-MWNTs) *f*-MWNTs across the PBEC co-culture model over a 72 h period. In general, higher percentage transport across PBEC was achieved for *w*-MWNTs compared with *t*-MWNTs (~15.6% and 7.6% of total dose after 72 h, respectively) [145]. Targeting of *f*-MWNTs was also tested in this study, in order to assess whether BBB translocation could be further improved. For this purpose, CNT synthesis was modified to incorporate a targeting peptide, angiopep-1 (ANG), to the carrier surface. This small peptide binds LRP1, a lipoprotein receptor that is overexpressed on brain endothelial cells of the BBB and several human tumours [147]. Indeed, higher values were obtained for ANG-functionalised *w*-MWNT and *t*-MWNTs (~20.3% and 11.6%, respectively) compared to the non-targeted carrier (~15.6% and 7.6%) [145], using the *in vitro* PBEC co-culture model. This confirmed that conjugation of this small LRP1-targeting peptide to *f*-CNT, enhances BBB

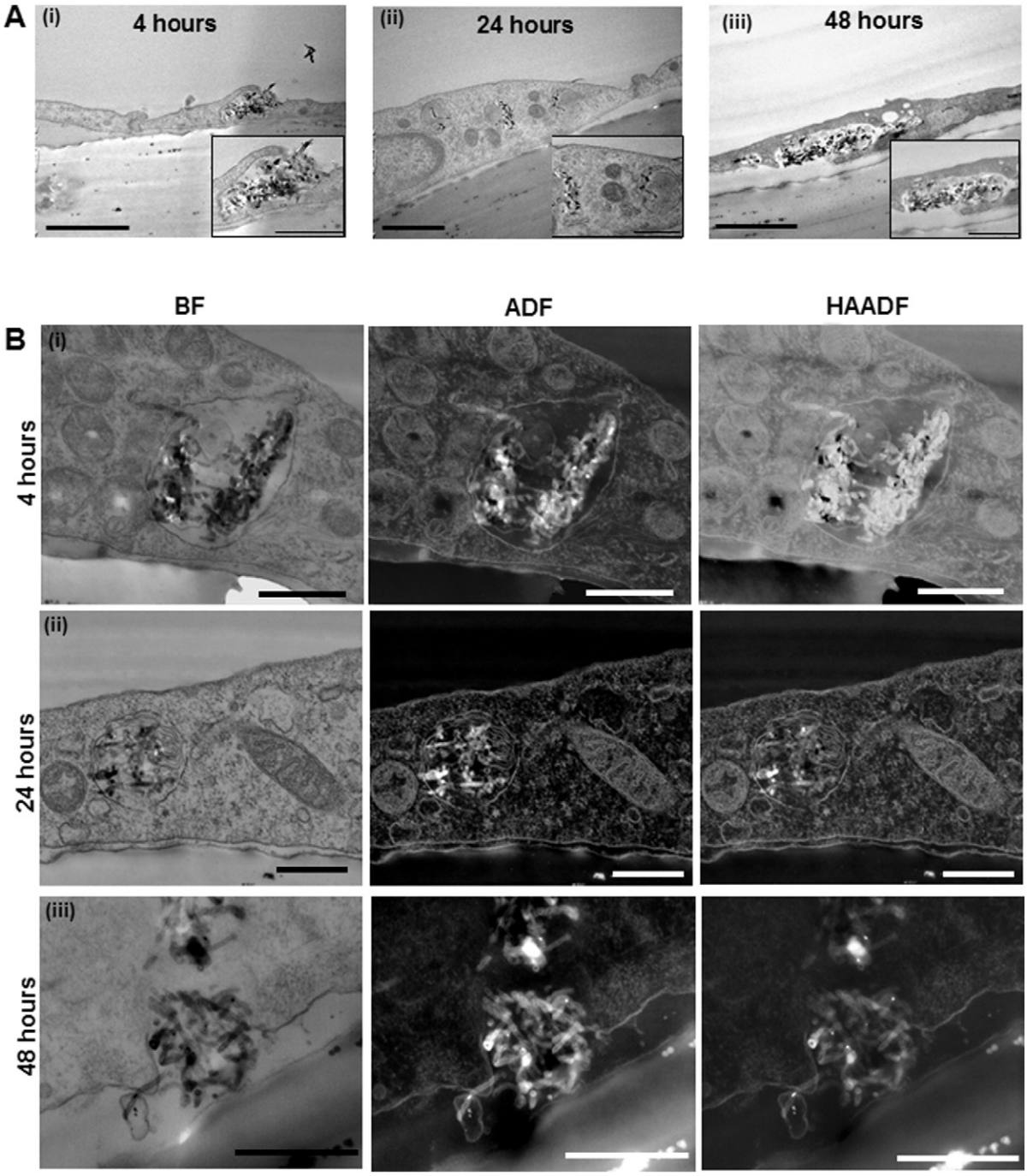

Fig. 6. Transcytosis of *f*-MWNTs across an *in vitro* BBB model. PBEC were incubated with MWNTs-NH_3^+ (20 μg/ml) for 4, 24 or 48 h. Cells were fixed in 2.5% glutaraldehyde for 24 h, before processing for imaging. (A) Bright field TEM and (B) low voltage STEM images of polyester filters showing the uptake and transcytosis of MWNTs-NH_3^+ across the PBEC monolayer. At 4 h, MWNTs-NH_3^+ clusters are seen interacting with the PBEC monolayer (or already within vesicles), while at 24 h the clusters appear within endocytic vesicles. At 48 h, the vesicles are seen partly opened towards the basal chamber to allow the release of vesicle contents. Scale bars: (A) 1 μm; inset: 500 nm. (B) 4 and 24 h: 500 nm; 48 h: 400 nm. BF: bright field; ADF: annular dark field; HAADF: high angular annular dark field. Figure reproduced from [144].

translocation and therefore could be of beneficial use for brain-targeted therapies.

The capacity of CNTs to cross the BBB *in vitro* without compromising this barrier was also demonstrated by Shityakov and colleagues. The authors used phase-contrast and fluorescence microscopy in combination with molecular dynamics simulation to demonstrate that amine-functionalised FITC-labelled MWNTs (MWCNT–NH_3^+–FITC) were able to penetrate murine microvascular cerebral endothelial (cEND) monolayers over a 48 h period, without compromising cell integrity [146].

5.2.2. In vivo BBB crossing

In addition to several *in vitro* studies, pre-clinical studies involving i.v. injection of CNTs provided unequivocal evidence of the capacity of CNTs to reach the tissues beyond the BBB.

In one of our very first studies, aiming at determining the impact of *f*-MWNT diameter on systemic organ biodistribution, it was revealed that radiolabelled *t*-MWNT conjugated to humanised IgG or fragment antigen binding region (Fab′) showed higher tissue affinity (including higher brain affinity) compared to *w*-MWNTs [148]. In a subsequent study, designed to investigate in detail the brain uptake, accumulation and elimination of *t*- and *w*-MWNTs (with or without ANG conjugation), following systemic administration in healthy mice [145], higher brain uptake was also found for *t*-MWNT (~2.6% ID/g tissue at 5 min) compared to *w*-MWNT (~1.1%) (Fig. 7). Importantly, ANG brain targeting effect was significant for *w*-MWNT-ANG (~2.0% *vs* 1.1%) but not for *t*-MWNT-ANG (~3.0% *vs* 2.6%). The capillary depletion method (which removes the vascular fraction of the brain), was then used to evaluate the *f*-MWNT content in the parenchyma and vascular brain fractions. Greater parenchyma uptake/accumulation was found for *t*-MWNTs compared to *w*-MWNTs, particularly at early times post-injection, while better parenchyma retention was found for *w*-MWNT conjugates. Negative elimination rate constants (Kel), indicating parenchyma

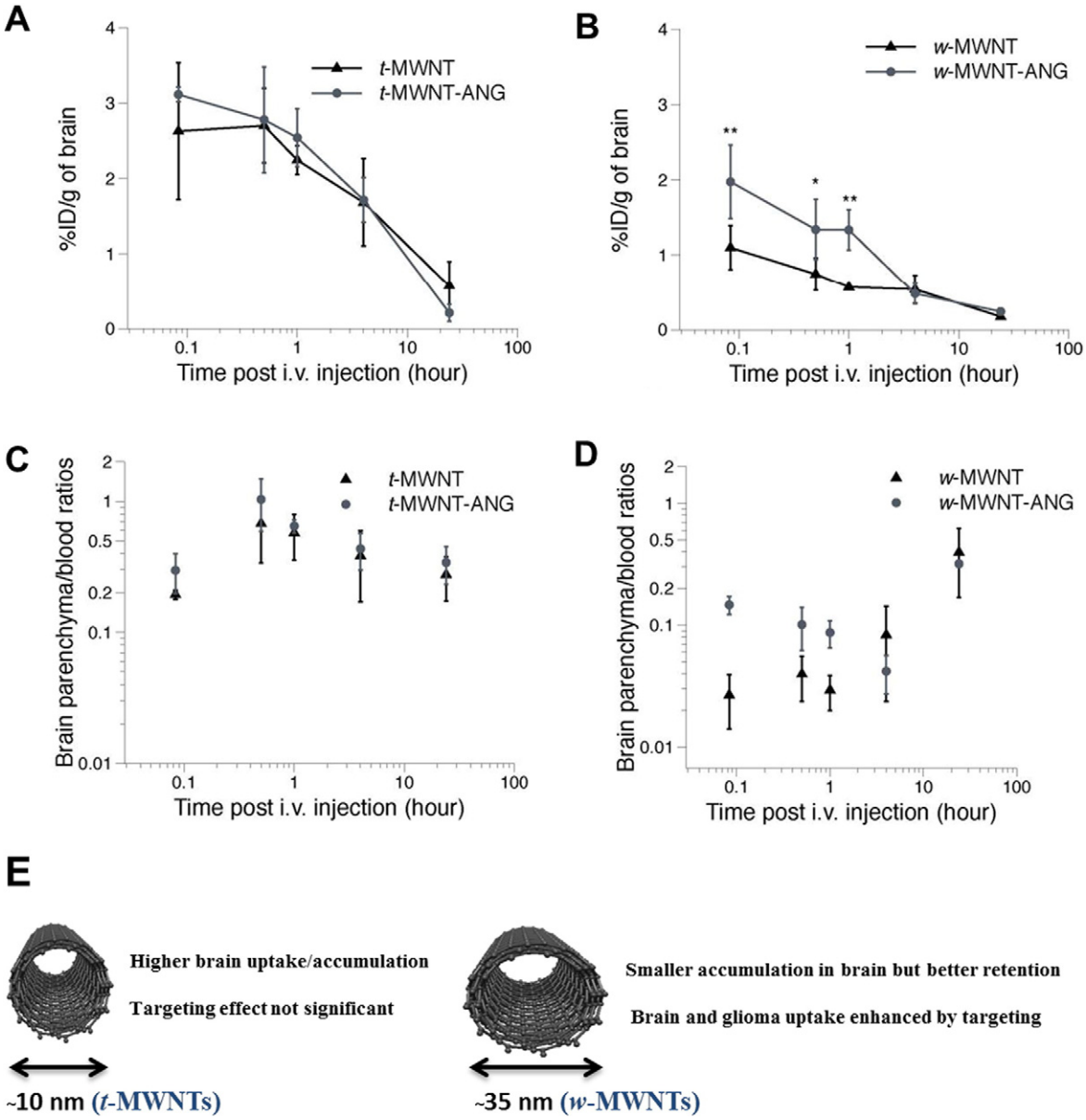

Fig. 7. Uptake of radiolabelled *f*-MWNTs into murine brain after systemic administration. C57BL/6 mice were injected, *via* tail vein, with wide (*w*-MWNT) or thin (*t*-MWNT) MWNTs (50 μg, 0.5 MBq). After perfusion with heparin-containing saline, brain accumulation was quantified by gamma scintigraphy, which was followed by capillary depletion at 5 min, 30 min, 1 h, 4 h and 24 h. The overall brain uptake of nontargeted and targeted (ANG-conjugated) (A) *t*-MWNTs or (B) *w*-MWNTs, expressed as % injected dose per gram of brain (%ID/g), revealed higher uptake for *t*-MWNTs. The radioactivity of (D) *t*-MWNTs or (D) *w*-MWNTs in brain parenchyma and capillaries, measured after capillary depletion, was used to calculate the brain parenchyma/blood ratios. $^{*}p < 0.05$; $^{**}p < 0.01$.
Adapted from [145].

retention, were obtained for *w*-MWNT and *w*-MWNTs-ANG (Kel ~ −0.026 and −0.05, respectively), compared to *t*-MWNT and *t*-MWNT-ANG which exhibited positive Kel values (~ 0.034 and ~0.019) suggesting elimination from parenchyma.

Since LRP1 overexpression has been described not only on brain endothelial cells but also for malignant brain tumours [147], experiments were also performed to investigate the capacity of i.v. injected ANG-coupled *w*-MWNTs, which show higher brain parenchyma retention, to target this type of tumour. Interestingly, *w*-MWNT-ANG not only showed significantly higher uptake in glioma when compared to normal brain, but also enhanced accumulation in glioma compared to the passively targeted *w*-MWNT [145], which suggests that ANG-coupling can provide a double-targeting effect, with improved brain and tumour uptake.

Overall, although *in vitro* data suggested that wider *f*-MWNTs are more efficient in crossing the BBB, the available *in vivo* data suggests that uptake in healthy brain tissues after systemic injection is favoured by *f*-MWNTs with smaller diameter, while wider MWNT exhibits better brain retention. ANG conjugation enhances brain uptake of wider MWNTs but offers no advantage to brain uptake of thinner ones. ANG-modified *f*-MWNT, of wider diameter, seems to be the most suitable candidate among the ones studied, for BBB and brain tumour double-targeting. Since the BBB-crossing studies were performed with "empty" CNTs, nevertheless, it is not known whether the % ID achieved is sufficient to generate a disease-specific response.

5.2.3. In vivo brain distribution

Following the encouraging results where *f*-MWNT achieved reasonably high brain parenchyma accumulation when delivered systemically, we used multi-modal imaging techniques to study in more detail the kinetics and spatial distribution of i.v. injected *f*-MWNTs in the brain [149]. SPECT/CT imaging clearly showed accumulation of radiolabelled *t*-MWNTs over the entire brain at the early time points after injection (5 min and 30 min), with higher radioactivity being detected in the mid-brain region (Fig. 8A). Autoradiography of brain slices (2 mm thick), which allows greater spatial resolution *via* increased exposure times and support of semi-quantitative analysis, provided further evidence of the preferential accumulation in the mid-brain region. Higher intensity was detected in sections of mid-brain (sections c3–5), while relatively lower radioactivity was detected in brain cortex (Fig. 8B). Importantly, gamma counting and TEM (Fig. 9A) showed preferential location of *t*-MWNTs in the brain capillaries up to 24 h after injection, which indicates that the MWNTs enter the brain *via* its endothelium. Moreover, TEM images showed that brain capillaries remained intact and circular, thus indicating that *t*-MWNT uptake into the brain was not caused by inflammation or the damage to the BBB.

Taking advantage of its inherent optical properties, *t*-MWNTs were also directly imaged in brain sections and whole brain using state-of-the-art techniques, namely Raman and multi-photon luminescence microscopy (Fig. 9B). The typical D (1309 cm^{-1}) and G (1599 cm^{-1}) MWNT Raman bands were seen in the spectra of capillaries (as well as in control bulk material), while no bands could be detected in whole brain sections. It is worth noting that *t*-MWNT accumulation in capillaries was ~4-fold higher than brain parenchyma. This highlights the limitation of this technique in terms of poor sensitivity.

5.2.4. In vivo brain-targeted therapy

While the above-mentioned studies investigated the BBB interaction, translocation and brain distribution of *f*-CNTs *in vivo*, they involved "empty" carriers. To date, very few studies investigated the delivery of CNT-formulated drugs to the brain following systemic administration.

Yang and colleagues used SWNTs for brain delivery of acetylcholine (ACh) to Alzheimer disease (AD)-bearing mice. In this regard, the administration of SWNTs-Ach, *via* oral gavage, resulted in improved learning and memory capabilities 8 h after treatment. Contrasting results were obtained in animals treated with empty SWNTs or the free Ach, in which no significant improvement was observed [150]. This study also highlighted the importance of the correct dosing of CNTs in brain-targeted therapies, as the mitochondria were shown to be affected by high concentrations of SWNTs. In a study by Ren and collaborators, PEGylated and carboxylated MWNTs (oxMWNT-PEG) modified with ANG were used as carrier to deliver doxorubicin to mouse brain. In addition to increased brain uptake of Dox-oxMWNT-PEG-ANG compared to Dox-oxMWNT-PEG or Dox *per se* after 1 to 6 h, the authors observed a substantial increase in survival of glioma-bearing animals treated with Dox-oxMWNT-PEG-ANG, compared to the saline-treated group [151]. Since fluorescence non-quantitative imaging was used to evaluate the doxorubicin dispersion in the brain, the accumulation rate of Dox-oxMWNT-PEG-ANG could not be compared to other delivery systems. Intravenously-injected NIR-fluorescent PEG-conjugated SWNT sensors,

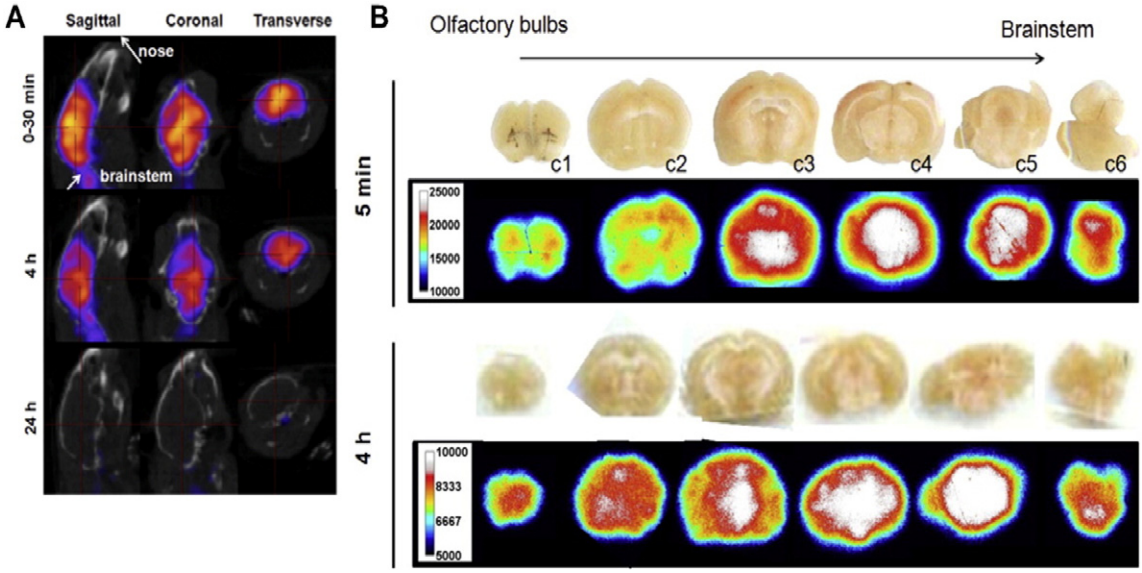

Fig. 8. Brain imaging after systemic administration of radiolabelled Fab′-conjugated *t*-MWNTs. C57BL/6 mice were administered 50 μg/ml of [^{111}In]MWNT-Fab′ *via* tail vein. (A) 3D reconstructed SPECT/CT images of mouse brains at 0–30 min, 4 h and 24 h post injection (0.5 MBq). (B) For autoradiography, brains were harvested at 5 min, 4 h or 24 h after i.v. injection (5–7 MBq) and 2 mm thick sections were prepared by coronal sectioning (from olfactory bulbs to brainstem). Sections were then analysed by autoradiography. Adapted from [149].

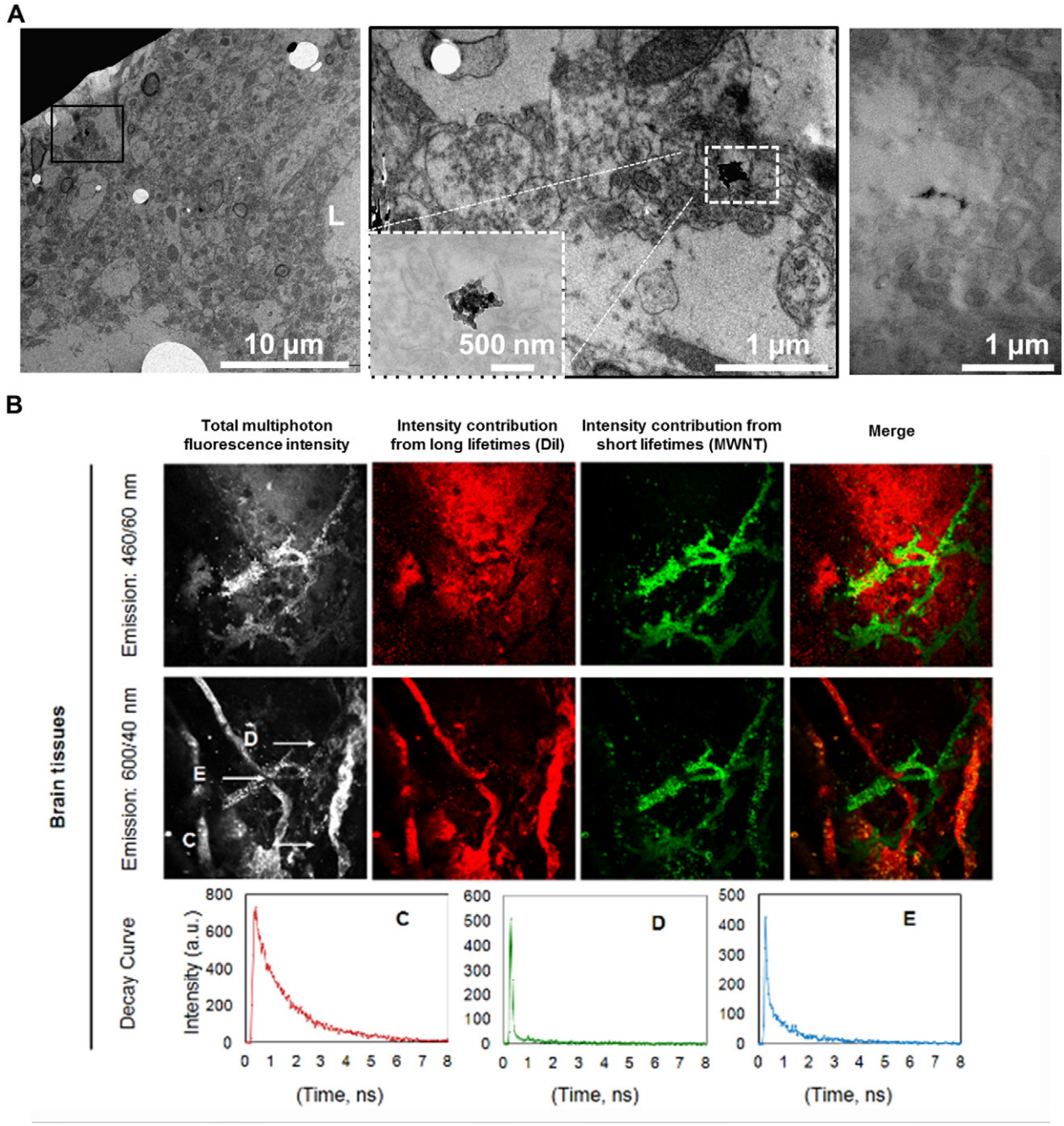

Fig. 9. Label-free brain imaging after systemic injection of Fab′-conjugated *t*-MWNTs. C57BL/6 mice were injected i.v. with MWNT-Fab′-DTPA (200 μg). (A) 5 min after injection mice were perfused with 2.5% glutaraldehyde (in 0.1 M cacodylate buffer), the brains were isolated and kept for another 24 h in fixation solution, before processing for TEM imaging. MWNT-Fab′-DTPA clusters are shown in the three different panels, including under higher magnification and enhanced contrast (middle panel, rectangular inlet). (B) For lifetime microscopy, the brains were isolated 1 h after injection (following perfusion with DiI and 4% PFA) and subsequently sectioned into 1 mm thick slices. Lifetime measurements are displayed below the multiphoton images (C, DiI; D, MWNT-Fab′-DTPA; E, position where both were present). Scale bar: 50 μm.
Adapted from [149].

developed by Iverson and colleagues, showed selective detection of local nitric oxide concentration in the brain, with a detection limit of 1 μM, with potential applications in sensing and therapy [152].

Table 3 summarizes the main studies involving local and systemic administration of CNT-based carriers for brain delivery, including carrier modifications, disease model and stage of development.

5.3. In vivo toxicity of CNTs in brain tissues

Cell and macromolecule traffic into the brain is strictly controlled by a tight BBB, efflux transporters and the presence of immune cells (microglia), to ensure a proper microenvironment in which neurons can function. Exposure to CNTs could disturb this fragile balance and result in cytotoxicity. No studies have yet assessed brain toxicity following systemic administration of CNTs. The evidence available, obtained from studies involving intracranial injection of nanotubes, suggests that surface functionalisation contributes to the cytotoxic outcome.

In a study by Bardi and colleagues, neuron toxicity was not detected in mouse brain cortex after stereotactic micro-injection of Pluronic® F-127 coated-MWNTs (MWNT:F127). Histological examination revealed small neuronal damaged near the injection site (due to the mechanical penetration of the brain) but no further damage was observed after

Table 3
Representative studies involving local or systemic administration of CNT-based nanocarriers for brain delivery.
List of abbreviations in this table: TMZ: temozolomide; SWNTs: single-walled carbon nanotubes; MWNTs: multi-walled carbon nanotubes; Ox-SWNT/MWNT: oxidised SWNT/MWNT; NIR: near infrared; NPCs: neural precursor cells; aSWNTs: aggregated SWNTs; METH: methamphetamine; NH_3^+-MWNTs: ammonium functionalized MWNTs; BBB: blood-brain barrier; Fab: fragment antigen binding region; ANG: angiopep1; *w*-MWNT: wide MWNT; *t*-MWNT: thin MWNT; AD: Alzheimer's disease; DOX: doxorubicin; NO: nitric oxide.

	CNT type and functionalisation	Therapeutic approach	Pre-clinical setting or disease model	Dosage	Main findings	Reference
Local administration	SWNT-PEG	Glioma immunotherapy - conjugation with CpG oligonucleotides	GL261 mouse glioma	Single intracranial injection (2.5 μg CNT/5 μg CpG)	Strong anti-tumoural response, decreased tumour size, increased median animal survival	[137]
	Ox-SWNT	Photothermal anti-glioma therapy	U251 TMZ-resistant mouse glioma	Single intratumoural injection (3 μg/ml) + single NIR laser treatment (10 min, 6.75 W/cm^2)	Suppression of tumour growth and inhibition of tumour recurrence for up to 80 days	[138]
	Commercially acquired CNTs	Stroke treatment - conjugation to neural precursor cells	Rat focal cerebral ischaemia (arterial occlusion)	Microinjection on the stroke area (striatum) of CNTs impregnated with 5×10^5 NPCs	Improved rat behaviour in neurological tests and reduced infarct cyst volume and area	[139]
	Ox-SWNTs	Stroke treatment	Rat focal cerebral ischaemia (arterial occlusion)	Pre-injection of 0.04 μg SWNTs onto the right lateral ventricle injection	Reduction in infarction area and improvement in behavioural functions	[140]
	NH_3^+-MWNTs	Stroke treatment - siRNA-mediated Caspase3 silencing	Mice and rat endothelin stroke model	Single intra-cortical injection of 0.5 μg NH_3^+-MWNTs	Decrease in apoptosis on the lesion area and improvement in behaviour tests	[142]
	a-SWNTs	METH addiction	Mouse model of METH self-administration	Pre-injection *via* cannula implanted on lateral ventricle, 1–2 μg SWNTs	Reduction in the rewarding and psycho-motor enhancing effects of METH	[141]
Systemic administration	MWNTs	BBB crossing studies - conjugation to IgG/Fab	Normal healthy mouse brain	"wide" (w) or "thin" (t) MWNTs, 50 μg injected *via* tail vein,	Higher brain affinity for *t*-MWNT compared to *w*-MWNT	[148]
	MWNTs	BBB crossing studies - conjugation to ANG	Normal healthy mouse brain and GL261 mouse glioma	*t*-MWNT/*w*-MWNT, 50 μg injected *via* tail vein	Higher brain uptake found for *t*-MWNTs (~2.6% ID/g tissue at 5 min) compared to *w*-MWNTs (~1.1%); Higher brain retention of *w*-MWNTs compared to *t*-MWNTs; Higher glioma uptake found for *w*-MWNTs-ANG	[145]
	Ox-MWNTs	Kinetics and distribution of CNTs in brain - conjugation to Fab	Normal healthy mouse brain	50 μg injected *via* tail vein	Accumulation of CNTs over entire brain early after injection, with preferential accumulation in the midbrain region	[149]
	SWNTs	Alzheimer's disease (AD) therapy - conjugation with acetylcholine (Ach)	Mouse model of AD (injection of kainic acid)	SWNT-Ach (25 mg/kg) administered by gastrogavage 24 h before injection of kainic acid	Improved learning and memory capabilities 8 h after treatment	[150]
	Ox-MWNT-PEG	Glioma chemotherapy – conjugation to ANG and DOX	C6 mouse glioma model	Dox-MWNT-PEG-ANG (1.5 mg DOX/0.375 mg MWNT) injected *via* tail vein at 2nd, 5th, 8th and 11th days after tumour implantation	Significant increase in animal survival	[151]
	SWNT-PEG-polymer	Biosensors for NO detection – conjugation to alginate	Normal healthy mouse brain	50 μg of alginate-encapsulated SWNT-PEG injected *via* tail vein	Selective detection of NO in the brain, with a detection limit of 1 μM	[152]

18 days [153]. In a previous manuscript from our group, it was shown that cortical stereotactic injection in mouse brain of MWNTs functionalised by 1,3-dipolar cycloaddition (MWNTs-NH_3^+) resulted in lower inflammation compared to the oxidised carrier (ox-MWNTs-NH_3^+) [154]. Similar uptake levels of the compounds were found in astrocytes, microglia and neurons, but a significantly higher release of the pro-inflammatory cytokines TNF-α and IL-1β, as well as microglia activation, was detected after injection of ox-MWNTs-NH_3^+ compared to MWNTs-NH_3^+. A recent follow-up study revealed that microglia is involved in the cytotoxic response generated by ox-MWNTs in brain tissue. Exposure of ox-MWNTs to neuronal cultures did not lead to detectable cytotoxicity (measured by the modified LDH assay), whereas significant cytotoxicity was found in mixed glial cultures isolated from striatum, but not from the frontal cortex. Striatum-derived mixed cultures contain a higher density of microglia, compared to the higher amount of astrocytes in the frontal cortex, thus suggesting that microglia is responsible for the CNTs-induced cytotoxicity in brain tissue [155].

5.4. Biodegradation of CNTs in brain tissues

The biodegradation of CNTs by brain cells has been studied *in vitro* and *in vivo*. Strong evidence suggests that CNTs can be degraded within human brain tissue by human MPO and hydrogen peroxide (H_2O_2).

Using Raman spectroscopy, Kagan and colleagues demonstrated that, in the presence of H_2O_2, MPO promoted SWNT biodegradation *via* generation of reactive hypochlorite radical intermediate species that oxidise parts of the CNT wall-structure [74]. Importantly, the presence of PEG (widely used to increase *in vivo* bioavailability) did

not interfere with this process. Biodegradation of oxidised and PEG-coated SWNTs (SWNTs-PEG) was observed after incubation for 7 days with MPO, H_2O_2 and NaCl. Further testing, carried out *ex vivo* using human neutrophils (which secrete MPO along with other proteases) showed efficient SWNTs-PEG degradation after only 8 h [74]. In a follow-up study, the biodegradation of SWNTs-PEG was proposed to occur in a two-step process, with the initial stripping of the PEG coating, mediated by secreted proteases, followed by SWNT degradation *via* surface defects [156]. Interestingly, PEG removal from the surface of SWNTs-PEG after systemic administration in mice has been previously described, but no explanation was provided for the mechanism [157].

In vivo data provides further evidence of the role of MPO on the CNT degradation in brain cells. Increased inflammation and lower SWNT clearance rate were detected in MPO mouse knockouts following pharyngeal aspiration, compared to wild type animals [75]. An elegant study by Nunes and colleagues, which used electron microscopy to assess degradation of stereotactically-administered *f*-MWNTs in mouse brain cortex, detected loss of cylindrical structure of *f*-MWNTs following internalisation into microglia [76]. The oxidative environment of the microglia, which contains MPO, peroxidases and other degradative enzymes, could be involved in the observed degradation.

Overall, the high surface area of CNTs, intrinsic capacity to cross the BBB, controlled toxicity and degradability in the presence of MPO enzymes are encouraging properties/observations for future applications of CNTs in the brain.

6. Concluding remarks and future perspectives

The progress achieved on the synthesis, design and functionalisation of carbon nanotubes has greatly contributed for the promising results obtained in *in vitro* and *in vivo* CNT-related studies. Surface modifications have improved carrier biocompatibility and targeting, while shortening CNT length improved pharmacokinetics and organ distribution. A wide range of *in vitro* studies has also revealed the mechanisms by which CNTs can lead to cell toxicity, including oxidative stress and mitochondrial dysfunction. Although a few studies have addressed the long-term biocompatibility and the effects of CNT accumulation in the human organs (namely the effects of pulmonary exposure) a higher number of long-term follow-up studies should aim at evaluating the long-term pharmacokinetics, organ accumulation, intracellular fate and possible cytotoxicity of intravenously-injected CNTs. The results of these studies will provide essential information about the behaviour of CNTs in complex physiological environment, allow the refinement of physicochemical and biocompatible properties and, ultimately, lead to the development of clinically-ready nanotube-based carriers. While research involving CNT-mediated therapeutic delivery to the brain has shown that biocompatible CNTs can efficiently reach the brain, little information is available about the amount of therapeutic molecule needed to obtain a significant therapeutic benefit. Future work should therefore focus on determining effective therapeutic disease-specific dosage, improving brain delivery and clarifying the fate of CNTs with the different CNS tissues, in healthy and diseased brain. This information would be extremely helpful for the design/production of improved *f*-CNT-based delivery systems that can, in the future, constitute primary options for efficient targeted brain therapy.

Acknowledgments

This work was supported by the Biotechnology and Biological Sciences Research Council [BB/J008656/1], EU FP7-ITN Marie-Curie Network programme RADDEL [290023] and Wellcome Trust [WT103913]. Pedro M. Costa is a Sir Henry Wellcome Post-doctoral fellow [WT103913]. Maxime Bourgognon is a Marie Curie Fellow.

References

[1] S. Iijima, Helical microtubules of graphitic carbon, Nature 354 (1991) 56–58, http://dx.doi.org/10.1038/354056a0.
[2] R.H. Baughman, A.A. Zakhidov, W.A. de Heer, Carbon nanotubes-the route toward applications, Science 297 (5582) (2002) 787–792, http://dx.doi.org/10.1126/science.1060928.
[3] A. Bianco, K. Kostarelos, C.D. Partidos, M. Prato, Biomedical applications of functionalised carbon nanotubes, Chem. Commun. (Camb.) (5) (2005) 571–577, http://dx.doi.org/10.1039/b410943k.
[4] A. Bianco, K. Kostarelos, M. Prato, Applications of carbon nanotubes in drug delivery, Curr. Opin. Chem. Biol. 9 (6) (2005) 674–679, http://dx.doi.org/10.1016/j.cbpa.2005.10.005.
[5] J. Kreuter, Nanoparticles - a historical perspective, Int. J. Pharm. 331 (1) (2007) 1–10, http://dx.doi.org/10.1016/j.ijpharm.2006.10.021.
[6] E. Heister, V. Neves, C. Tîlmaciu, K. Lipert, V.S. Beltrán, H.M. Coley, S.R.P. Silva, J. McFadden, Triple functionalisation of single-walled carbon nanotubes with doxorubicin, a monoclonal antibody, and a fluorescent marker for targeted cancer therapy, Carbon 47 (9) (2009) 2152–2160.
[7] C.L. Lay, H.Q. Liu, H.R. Tan, Y. Liu, Delivery of paclitaxel by physically loading onto poly(ethylene glycol) (PEG)-graft-carbon nanotubes for potent cancer therapeutics, Nanotechnology 21 (6) (2010) 065101, http://dx.doi.org/10.1088/0957-4484/21/6/065101.
[8] A. Peigney, C. Laurent, E. Flahaut, R.R. Bacsa, A. Rousset, Specific surface area of carbon nanotubes and bundles of carbon nanotubes, Carbon 39 (4) (2001) 507–514, http://dx.doi.org/10.1016/S0008-6223(00)00155-X.
[9] D. Pantarotto, R. Singh, D. McCarthy, M. Erhardt, J.P. Briand, M. Prato, K. Kostarelos, A. Bianco, Functionalized carbon nanotubes for plasmid DNA gene delivery, Angew. Chem. Int. Ed. Engl. 43 (39) (2004) 5242–5246.
[10] C.A. Poland, R. Duffin, I. Kinloch, A. Maynard, W.A. Wallace, A. Seaton, V. Stone, S. Brown, W. Macnee, K. Donaldson, Carbon nanotubes introduced into the abdominal cavity of mice show asbestos-like pathogenicity in a pilot study, Nat. Nanotechnol. 3 (7) (2008) 423–428, http://dx.doi.org/10.1038/nnano.2008.111.
[11] S. Lanone, P. Andujar, A. Kermanizadeh, J. Boczkowski, Determinants of carbon nanotube toxicity, Adv. Drug Deliv. Rev. 65 (15) (2013) 2063–2069, http://dx.doi.org/10.1016/j.addr.2013.07.019.
[12] H. Dumortier, S. Lacotte, G. Pastorin, R. Marega, W. Wu, D. Bonifazi, J.P. Briand, M. Prato, S. Muller, A. Bianco, Functionalized carbon nanotubes are non-cytotoxic and preserve the functionality of primary immune cells, Nano Lett. 6 (7) (2006) 1522–1528 (Erratum in: Nano Lett. 2006;6(12):3003).
[13] A. Hirsch, O. Vostrowsky, Functionalization of carbon nanotubes, Top. Curr. Chem. 243 (2005) 193–237, http://dx.doi.org/10.1007/b98169.
[14] P.C. Ma, N.A. Siddiqui, G. Marom, J.K. Kim, Dispersion and functionalization of carbon nanotubes for polymer-based nanocomposites: a review, Compos. A: Appl. Sci. Manuf. 41 (10) (2010) 1345–1367, http://dx.doi.org/10.1016/j.compositesa.2010.07.003.
[15] R. Marega, D. Bonifazi, Filling carbon nanotubes for nanobiotechnological applications, New J. Chem. 38 (1) (2014) 22–27, http://dx.doi.org/10.1039/C3NJ01008B.
[16] H. Gong, R. Peng, Z. Liu, Carbon nanotubes for biomedical imaging: the recent advances, Adv. Drug Deliv. Rev. 65 (15) (2013) 1951–1963, http://dx.doi.org/10.1016/j.addr.2013.10.002.
[17] A. Ruggiero, C.H. Villa, J.P. Holland, S.R. Sprinkle, C. May, J.S. Lewis, D.A. Scheinberg, M.R. McDevitt, Imaging and treating tumor vasculature with targeted radiolabeled carbon nanotubes, Int. J. Nanomedicine 5 (2010) 783–802, http://dx.doi.org/10.2147/IJN.S13300.
[18] H. Wu, H. Shi, H. Zhang, X. Wang, Y. Yang, C. Yu, C. Hao, J. Du, H. Hu, S. Yang, Prostate stem cell antigen antibody-conjugated multiwalled carbon nanotubes for targeted ultrasound imaging and drug delivery, Biomaterials 35 (20) (2014) 5369–5380, http://dx.doi.org/10.1016/j.biomaterials.2014.03.038.
[19] K.T. Al-Jamal, A. Nunes, L. Methven, H. Ali-Boucetta, S. Li, F.M. Toma, M.A. Herrero, W.T. Al-Jamal, H.M. ten Eikelder, J. Foster, S. Mather, M. Prato, A. Bianco, K. Kostarelos, Degree of chemical functionalization of carbon nanotubes determines tissue distribution and excretion profile, Angew. Chem. Int. Ed. Engl. 51 (26) (2012) 6389–6393, http://dx.doi.org/10.1002/anie.201201991.
[20] D.E. Lee, H. Koo, I.C. Sun, J.H. Ryu, K. Kim, I.C. Kwon, Multifunctional nanoparticles for multimodal imaging and theragnosis, Chem. Soc. Rev. 41 (7) (2012) 2656–2672, http://dx.doi.org/10.1039/c2cs15261d.
[21] J.T. Wang, K.T. Al-Jamal, Functionalized carbon nanotubes: revolution in brain delivery, Nanomedicine (Lond.) 10 (17) (2015) 2639–2642, http://dx.doi.org/10.2217/nnm.15.114.
[22] C. Journet, W. Maser, P. Bernier, Large-scale production of single-walled carbon nanotubes by the electric-arc technique, Nature 388 (1997) 756–758.
[23] C.D. Scott, S. Arepalli, P. Nikolaev, R.E. Smalley, Growth mechanisms for single-wall carbon nanotubes in a laser-ablation process, Appl. Phys. A Mater. Sci. Process. 72 (2001) 573–580, http://dx.doi.org/10.1007/s003390100761.
[24] Z.P. Huang, J.W. Xu, Z.F. Ren, J.H. Wang, M.P. Siegal, P.N. Provencio, Growth of highly oriented carbon nanotubes by plasma-enhanced hot filament chemical vapor deposition, Appl. Phys. Lett. 73 (1998) 3845, http://dx.doi.org/10.1063/1.122912.
[25] A. Hirsch, Funktionalisierung von einwandigen Kohlenstoffnanoröhren, Angew. Chem. 114 (11) (2002) 1933–1939.
[26] S. Iijima, Carbon nanotubes: past, present, and future, Phys. B Condens. Matter 323 (4) (2002) 1–5, http://dx.doi.org/10.1016/S0921-4526(02)00869-4.
[27] B. Ballesteros, G. Tobias, L. Shao, E. Pellicer, J. Nogués, E. Mendoza, M.L. Green, Steam purification for the removal of graphitic shells coating catalytic particles and the shortening of single-walled carbon nanotubes, Small 4 (9) (2008) 1501–1506, http://dx.doi.org/10.1002/smll.200701283.

[28] C. Bussy, M. Pinault, J. Cambedouzou, M.J. Landry, P. Jegou, M. Mayne-L'hermite, P. Launois, J. Boczkowski, S. Lanone, Critical role of surface chemical modifications induced by length shortening on multi-walled carbon nanotubes-induced toxicity, Part. Fibre Toxicol. 9 (2012) 46, http://dx.doi.org/10.1186/1743-8977-9-46.
[29] N. Rubio, C. Fabbro, M.A. Herrero, A. de la Hoz, M. Meneghetti, J.L. Fierro, M. Prato, E. Vázquez, Ball-milling modification of single-walled carbon nanotubes: purification, cutting, and functionalization, Small 7 (5) (2011) 665–674, http://dx.doi.org/10.1002/smll.201001917.
[30] Z. Liu, S. Tabakman, K. Welsher, H. Dai, Carbon nanotubes in biology and medicine: in vitro and in vivo detection, imaging and drug delivery, Nano Res. 2 (2) (2009) 85–120, http://dx.doi.org/10.1007/s12274-009-9009-8.
[31] B. Koh, W. Cheng, Mechanisms of carbon nanotube aggregation and the reversion of carbon nanotube aggregates in aqueous medium, Langmuir 30 (36) (2014) 10899–10909, http://dx.doi.org/10.1021/la5014279.
[32] R.J. Chen, Y. Zhang, D. Wang, H. Dai, Noncovalent sidewall functionalization of single-walled carbon nanotubes for protein immobilization, J. Am. Chem. Soc. 123 (16) (2001) 3838–3839, http://dx.doi.org/10.1021/ja010172b.
[33] N. Grossiord, P. Schoot, J. Meuldijk, C.E. Koning, Determination of the surface coverage of exfoliated carbon nanotubes by surfactant molecules in aqueous solution, Langmuir 23 (2007) 3646–3653, http://dx.doi.org/10.1021/la062684f.
[34] M.C. Hersam, Progress towards monodisperse single-walled carbon nanotubes, Nat. Nanotechnol. 3 (7) (2008) 387–394, http://dx.doi.org/10.1038/nnano.2008.135.
[35] J.U. Lee, J. Huh, K.H. Kim, C. Park, W.H. Jo, Aqueous suspension of carbon nanotubes via non-covalent functionalization with oligothiophene-terminated poly(ethylene glycol), Carbon 45 (2007) 1051–1057, http://dx.doi.org/10.1016/j.carbon.2006.12.017.
[36] N.A. Monteiro-Riviere, A.O. Inman, Y.Y. Wang, R.J. Nemanich, Surfactant effects on carbon nanotube interactions with human keratinocytes, Nanomedicine 1 (4) (2005) 293–299, http://dx.doi.org/10.1016/j.nano.2005.10.007.
[37] A.L. Alpatova, W. Shan, P. Babica, B.L. Upham, A.R. Rogensues, S.J. Masten, E. Drown, A.K. Mohanty, E.C. Alocilja, V.V. Tarabara, Single-walled carbon nanotubes dispersed in aqueous media via non-covalent functionalization: effect of dispersant on the stability, cytotoxicity, and epigenetic toxicity of nanotube suspensions, Water Res. 44 (2) (2010) 505–520, http://dx.doi.org/10.1016/j.watres.2009.09.042.
[38] M. Zheng, A. Jagota, E.D. Semke, B.A. Diner, R.S. McLean, S.R. Lustig, R.E. Richardson, N.G. Tassi, DNA-assisted dispersion and separation of carbon nanotubes, Nat. Mater. 2 (5) (2003) 338–342, http://dx.doi.org/10.1038/nmat877.
[39] E. Edri, O. Regev, "Shaken, not stable": dispersion mechanism and dynamics of protein-dispersed nanotubes studied via spectroscopy, Langmuir 25 (18) (2009) 10459–10465, http://dx.doi.org/10.1021/la901386y.
[40] A.E. Frise, E. Edri, I. Furó, O. Regev, Protein dispersant binding on nanotubes studied by NMR self-diffusion and cryo-TEM techniques, J. Phys. Chem. Lett. 1 (2010) 1414–1419, http://dx.doi.org/10.1021/jz100342c.
[41] M. Foldvari, M. Bagonluri, Carbon nanotubes as functional excipients for nanomedicines: II. Drug delivery and biocompatibility issues, Nanomedicine 4 (3) (2008) 183–200, http://dx.doi.org/10.1016/j.nano.2008.04.003.
[42] P. Singh, S. Campidelli, S. Giordani, D. Bonifazi, A. Bianco, M. Prato, Organic functionalisation and characterisation of single-walled carbon nanotubes, Chem. Soc. Rev. 38 (8) (2009) 2214–2230, http://dx.doi.org/10.1039/b518111a.
[43] M.N. Kirikova, A.S. Ivanov, S.V. Savilov, V.V. Lunin, Modification of multiwalled carbon nanotubes by carboxy groups and determination of the degree of functionalization, Russ. Chem. Bull. 57 (2009) 298–303, http://dx.doi.org/10.1007/s11172-008-0046-3.
[44] A. Fraczek-Szczypta, E. Menaszek, T.B. Syeda, A. Misra, M. Alavijeh, J. Adu, S. Blazewicz, Effect of MWCNT surface and chemical modification on in vitro cellular response, J. Nanopart. Res. 14 (10) (2012) 1181, http://dx.doi.org/10.1007/s11051-012-1181-1.
[45] V. Georgakilas, K. Kordatos, M. Prato, D.M. Guldi, M. Holzinger, A. Hirsch, Organic functionalization of carbon nanotubes, J. Am. Chem. Soc. 124 (5) (2002) 760–761, http://dx.doi.org/10.1021/ja016954m.
[46] H. Jin, D.A. Heller, M.S. Strano, Single-particle tracking of endocytosis and exocytosis of single-walled carbon nanotubes in NIH-3T3 cells, Nano Lett. 8 (6) (2008) 1577–1585, http://dx.doi.org/10.1021/nl072969s.
[47] H. Jin, D.A. Heller, R. Sharma, M.S. Strano, Size-dependent cellular uptake and expulsion of single-walled carbon nanotubes: single particle tracking and a generic uptake model for nanoparticles, ACS Nano 3 (1) (2009) 149–158, http://dx.doi.org/10.1021/nn800532m.
[48] V.E. Kagan, A.A. Kapralov, C.M. St Croix, S.C. Watkins, E.R. Kisin, G.P. Kotchey, K. Balasubramanian, I.I. Vlasova, J. Yu, K. Kim, W. Seo, R.K. Mallampalli, A. Star, A.A. Shvedova, Lung macrophages "digest" carbon nanotubes using a superoxide/peroxynitrite oxidative pathway, ACS Nano 8 (6) (2014) 5610–5621, http://dx.doi.org/10.1021/nn406484b.
[49] B. Kang, J. Li, S. Chang, M. Dai, C. Ren, Y. Dai, D. Chen, Subcellular tracking of drug release from carbon nanotube vehicles in living cells, Small 8 (5) (2012) 777–782, http://dx.doi.org/10.1002/smll.201101714.
[50] A.A. Shvedova, A. Pietroiusti, B. Fadeel, V.E. Kagan, Mechanisms of carbon nanotube-induced toxicity: focus on oxidative stress, Toxicol. Appl. Pharmacol. 261 (2) (2012) 121–133, http://dx.doi.org/10.1016/j.taap.2012.03.023.
[51] Q. Mu, D.L. Broughton, B. Yan, Endosomal leakage and nuclear translocation of multiwalled carbon nanotubes: developing a model for cell uptake, Nano Lett. 9 (12) (2009) 4370–4375, http://dx.doi.org/10.1021/nl902647x.
[52] N.W. Shi Kam, T.C. Jessop, P.A. Wender, H. Dai, Nanotube molecular transporters: internalization of carbon nanotube-protein conjugates into mammalian cells, J. Am. Chem. Soc. 126 (22) (2004) 6850–6851, http://dx.doi.org/10.1021/ja0486059.
[53] N.W. Kam, H. Dai, Carbon nanotubes as intracellular protein transporters: generality and biological functionality, J. Am. Chem. Soc. 127 (16) (2005) 6021–6026, http://dx.doi.org/10.1021/ja050062v.
[54] M. Wang, S. Yu, C. Wang, J. Kong, Tracking the endocytic pathway of recombinant protein toxin delivered by multiwalled carbon nanotubes, ACS Nano 4 (11) (2010) 6483–6490, http://dx.doi.org/10.1021/nn101445y.
[55] X. Shi, A. von dem Bussche, R.H. Hurt, A.B. Kane, H. Gao, Cell entry of one-dimensional nanomaterials occurs by tip recognition and rotation, Nat. Nanotechnol. 6 (11) (2011) 714–719, http://dx.doi.org/10.1038/nnano.2011.151.
[56] S. Kraszewski, A. Bianco, M. Tarek, C. Ramseyer, Insertion of short amino-functionalized single-walled carbon nanotubes into phospholipid bilayer occurs by passive diffusion, PLoS One 7 (7) (2012), e40703 http://dx.doi.org/10.1371/journal.pone.0040703.
[57] L. Lacerda, H. Ali-Boucetta, S. Kraszewski, M. Tarek, M. Prato, C. Ramseyer, K. Kostarelos, A. Bianco, How do functionalized carbon nanotubes land on, bind to and pierce through model and plasma membranes, Nanoscale 5 (21) (2013) 10242–10250, http://dx.doi.org/10.1039/c3nr03184e.
[58] L. Lacerda, H. Ali-Boucetta, M.A. Herrero, G. Pastorin, A. Bianco, M. Prato, K. Kostarelos, Tissue histology and physiology following intravenous administration of different types of functionalized multiwalled carbon nanotubes, Nanomedicine (Lond.) 3 (2) (2008) 149–161, http://dx.doi.org/10.2217/17435889.3.2.149.
[59] R.A. Petros, J.M. DeSimone, Strategies in the design of nanoparticles for therapeutic applications, Nat. Rev. Drug Discov. 9 (8) (2010) 615–627, http://dx.doi.org/10.1038/nrd2591.
[60] Q. Wei, L. Zhan, B. Juanjuan, W. Jing, W. Jianjun, S. Taoli, G. Yi'an, W. Wangsuo, Biodistribution of co-exposure to multi-walled carbon nanotubes and nanodiamonds in mice, Nanoscale Res. Lett. 7 (1) (2012) 473, http://dx.doi.org/10.1186/1556-276X-7-473.
[61] K.T. Al-Jamal, H. Nerl, K.H. Müller, H. Ali-Boucetta, S. Li, P.D. Haynes, J.R. Jinschek, M. Prato, A. Bianco, K. Kostarelos, A.E. Porter, Cellular uptake mechanisms of functionalised multi-walled carbon nanotubes by 3D electron tomography imaging, Nanoscale 3 (6) (2011) 2627–2635, http://dx.doi.org/10.1039/c1nr10080g.
[62] F. Zhou, D. Xing, B. Wu, S. Wu, Z. Ou, W.R. Chen, New insights of transmembranal mechanism and subcellular localization of noncovalently modified single-walled carbon nanotubes, Nano Lett. 10 (5) (2010) 1677–1681, http://dx.doi.org/10.1021/nl100004m.
[63] A. Antonelli, S. Serafini, M. Menotta, C. Sfara, F. Pierigé, L. Giorgi, G. Ambrosi, L. Rossi, M. Magnani, Improved cellular uptake of functionalized single-walled carbon nanotubes, Nanotechnology 21 (42) (2010) 425101, http://dx.doi.org/10.1088/0957-4484/21/42/425101.
[64] V. Neves, A. Gerondopoulos, E. Heister, C. Tîlmaciu, E. Flahaut, B. Soula, S.R.P. Silva, J. McFadden, H.M. Coley, Cellular localization, accumulation and trafficking of double-walled carbon nanotubes in human prostate cancer cells, Nano Res. 5 (4) (2012) 223–234, http://dx.doi.org/10.1007/s12274-012-0202-9.
[65] L. Lacerda, G. Pastorin, D. Gathercole, J. Buddle, M. Prato, A. Bianco, K. Kostarelos, Intracellular trafficking of carbon nanotubes by confocal laser scanning microscopy, Adv. Mater. 19 (11) (2007) 1480–1484, http://dx.doi.org/10.1002/adma.200601412.
[66] F. Zhou, S. Wu, Y. Yuan, W.R. Chen, D. Xing, Mitochondria-targeting photoacoustic therapy using single-walled carbon nanotubes, Small 8 (10) (2012) 1543–1550, http://dx.doi.org/10.1002/smll.201101892.
[67] V. Neves, E. Heister, S. Costa, C. Tîlmaciu, E. Borowiak-Palen, C.E. Giusca, E. Flahaut, B. Soula, H.M. Coley, J. McFadden, S.R.P. Silva, Uptake and release of double-walled carbon nanotubes by mammalian cells, Adv. Funct. Mater. 20 (2010) 3272–3279, http://dx.doi.org/10.1002/adfm.201000994.
[68] I. Marangon, N. Boggetto, C. Ménard-Moyon, E. Venturelli, M.L. Béoutis, C. Péchoux, N. Luciani, C. Wilhelm, A. Bianco, F. Gazeau, Intercellular carbon nanotube translocation assessed by flow cytometry imaging, Nano Lett. 12 (9) (2012) 4830–4837, http://dx.doi.org/10.1021/nl302273p.
[69] M. Orecna, S.H. De Paoli, O. Janouskova, T.Z. Tegegn, M. Filipova, J.E. Bonevich, K. Holada, J. Simak, Toxicity of carboxylated carbon nanotubes in endothelial cells is attenuated by stimulation of the autophagic flux with the release of nanomaterial in autophagic vesicles, Nanomedicine 10 (5) (2014) 939–948, http://dx.doi.org/10.1016/j.nano.2014.02.001.
[70] B.L. Allen, P.D. Kichambare, P. Gou, I.I. Vlasova, A.A. Kapralov, N. Konduru, V.E. Kagan, A. Star, Biodegradation of single-walled carbon nanotubes through enzymatic catalysis, Nano Lett. 8 (11) (2008) 3899–3903, http://dx.doi.org/10.1021/nl802315h.
[71] B.L. Allen, G.P. Kotchey, Y. Chen, N.V. Yanamala, J. Klein-Seetharaman, V.E. Kagan, A. Star, Mechanistic investigations of horseradish peroxidase-catalyzed degradation of single-walled carbon nanotubes, J. Am. Chem. Soc. 131 (47) (2009) 17194–17205, http://dx.doi.org/10.1021/ja9083623.
[72] Y. Zhao, B.L. Allen, A. Star, Enzymatic degradation of multiwalled carbon nanotubes, J. Phys. Chem. A 115 (34) (2011) 9536–9544, http://dx.doi.org/10.1021/jp112324d.
[73] C. Farrera, K. Bhattacharya, B. Lazzaretto, F.T. Andón, K. Hultenby, G.P. Kotchey, A. Star, B. Fadeel, Extracellular entrapment and degradation of single-walled carbon nanotubes, Nanoscale 6 (12) (2014) 6974–6983, http://dx.doi.org/10.1039/c3nr06047k.
[74] V.E. Kagan, N.V. Konduru, W. Feng, B.L. Allen, J. Conroy, Y. Volkov, I.I. Vlasova, N.A. Belikova, N. Yanamala, A. Kapralov, Y.Y. Tyurina, J. Shi, E.R. Kisin, A.R. Murray, J. Franks, D. Stolz, P. Gou, J. Klein-Seetharaman, B. Fadeel, A. Star, A.A. Shvedova, Carbon nanotubes degraded by neutrophil myeloperoxidase induce less pulmonary inflammation, Nat. Nanotechnol. 5 (5) (2010) 354–359, http://dx.doi.org/10.1038/nnano.2010.44.

[75] A.A. Shvedova, A.A. Kapralov, W.H. Feng, E.R. Kisin, A.R. Murray, R.R. Mercer, C.M. St Croix, M.A. Lang, S.C. Watkins, N.V. Konduru, B.L. Allen, J. Conroy, G.P. Kotchey, B.M. Mohamed, A.D. Meade, Y. Volkov, A. Star, B. Fadeel, V.E. Kagan, Impaired clearance and enhanced pulmonary inflammatory/fibrotic response to carbon nanotubes in myeloperoxidase-deficient mice, PLoS One 7 (3) (2012), e30923 http://dx.doi.org/10.1371/journal.pone.0030923.

[76] A. Nunes, C. Bussy, L. Gherardini, M. Meneghetti, M.A. Herrero, A. Bianco, M. Prato, T. Pizzorusso, K.T. Al-Jamal, K. Kostarelos, In vivo degradation of functionalized carbon nanotubes after stereotactic administration in the brain cortex, Nanomedicine (Lond.) 7 (10) (2012) 1485–1494, http://dx.doi.org/10.2217/nnm.12.33.

[77] D.X. Flores-Cervantes, H.M. Maes, A. Schäffer, J. Hollender, H.P. Kohler, Slow biotransformation of carbon nanotubes by horseradish peroxidase, Environ. Sci. Technol. 48 (9) (2014) 4826–4834, http://dx.doi.org/10.1021/es4053279.

[78] C.W. Lam, J.T. James, R. McCluskey, S. Arepalli, R.L. Hunter, A review of carbon nanotube toxicity and assessment of potential occupational and environmental health risks, Crit. Rev. Toxicol. 36 (3) (2006) 189–217.

[79] A. Nel, T. Xia, L. Mädler, N. Li, Toxic potential of materials at the nanolevel, Science 311 (5761) (2006) 622–627, http://dx.doi.org/10.1126/science.1114397.

[80] L. Gonzalez, D. Lison, M. Kirsch-Volders, Genotoxicity of engineered nanomaterials: a critical review, Nanotoxicology 2 (4) (2008) 252–273, http://dx.doi.org/10.1080/17435390802464986.

[81] C.M. Sayes, A.M. Gobin, K.D. Ausman, J. Mendez, J.L. West, V.L. Colvin, Nano-C60 cytotoxicity is due to lipid peroxidation, Biomaterials 26 (36) (2005) 7587–7595, http://dx.doi.org/10.1016/j.biomaterials.2005.05.027.

[82] V. Vallyathan, X. Shi, The role of oxygen free radicals in occupational and environmental lung diseases, Environ. Health Perspect. 105 (Suppl 1) (1997) 165–177, http://dx.doi.org/10.2307/3433405.

[83] M.D. Jacobson, Reactive oxygen species and programmed cell death, Trends Biochem. Sci. 21 (3) (1996) 83–86, http://dx.doi.org/10.1016/S0968-0004(96)20008-8.

[84] J. Muller, F. Huaux, A. Fonseca, J.B. Nagy, N. Moreau, M. Delos, E. Raymundo-Piñero, F. Béguin, M. Kirsch-Volders, I. Fenoglio, B. Fubini, D. Lison, Structural defects play a major role in the acute lung toxicity of multiwall carbon nanotubes: toxicological aspects, Chem. Res. Toxicol. 21 (9) (2008) 1698–1705, http://dx.doi.org/10.1021/tx800101p.

[85] G.G. Xiao, M. Wang, N. Li, J.A. Loo, A.E. Nel, Use of proteomics to demonstrate a hierarchical oxidative stress response to diesel exhaust particle chemicals in a macrophage cell line, J. Biol. Chem. 278 (50) (2003) 50781–50790, http://dx.doi.org/10.1074/jbc.M306423200.

[86] V.E. Kagan, Y.Y. Tyurina, V.A. Tyurin, N.V. Konduru, A.I. Potapovich, A.N. Osipov, E.R. Kisin, D. Schwegler-Berry, R. Mercer, V. Castranova, A.A. Shvedova, Direct and indirect effects of single walled carbon nanotubes on RAW 264.7 macrophages: role of iron, Toxicol. Lett. 165 (1) (2006) 88–100, http://dx.doi.org/10.1016/j.toxlet.2006.02.001.

[87] L. Meng, A. Jiang, R. Chen, C.Z. Li, L. Wang, Y. Qu, P. Wang, Y. Zhao, C. Chen, Inhibitory effects of multiwall carbon nanotubes with high iron impurity on viability and neuronal differentiation in cultured PC12 cells, Toxicology 313 (1) (2013) 49–58, http://dx.doi.org/10.1016/j.tox.2012.11.011.

[88] E. Aldieri, I. Fenoglio, F. Cesano, E. Gazzano, G. Gulino, D. Scarano, A. Attanasio, G. Mazzucco, D. Ghigo, B. Fubini, The role of iron impurities in the toxic effects exerted by short multiwalled carbon nanotubes (MWCNT) in murine alveolar macrophages, J. Toxicol. Environ. Health A 76 (18) (2013) 1056–1071, http://dx.doi.org/10.1080/15287394.2013.834855.

[89] R.F. Hamilton Jr., M. Buford, C. Xiang, N. Wu, A. Holian, NLRP3 inflammasome activation in murine alveolar macrophages and related lung pathology is associated with MWCNT nickel contamination, Inhal. Toxicol. 24 (14) (2012) 995–1008, http://dx.doi.org/10.3109/08958378.2012.745633.

[90] A. Simon-Deckers, B. Gouget, M. Mayne-L'hermite, N. Herlin-Boime, C. Reynaud, M. Carrière, In vitro investigation of oxide nanoparticle and carbon nanotube toxicity and intracellular accumulation in A549 human pneumocytes, Toxicology 253 (1–3) (2008) 137–146, http://dx.doi.org/10.1016/j.tox.2008.09.007.

[91] H.J. Patel, S. Kwon, Length-dependent effect of single-walled carbon nanotube exposure in a dynamic cell growth environment of human alveolar epithelial cells, J. Expo. Sci. Environ. Epidemiol. 23 (1) (2013) 101–108, http://dx.doi.org/10.1038/jes.2012.75.

[92] S. Sweeney, D. Berhanu, S.K. Misra, A.J. Thorley, E. Valsami-Jones, T.D. Tetley, Multiwalled carbon nanotube length as a critical determinant of bioreactivity with primary human pulmonary alveolar cells, Carbon N Y. 78 (2014) 26–37, http://dx.doi.org/10.1016/j.carbon.2014.06.033.

[93] D. Liu, L. Wang, Z. Wang, A. Cuschieri, Different cellular response mechanisms contribute to the length-dependent cytotoxicity of multi-walled carbon nanotubes, Nanoscale Res. Lett. 7 (1) (2012) 361, http://dx.doi.org/10.1186/1556-276X-7-361.

[94] J.S. Kim, K. Lee, Y.H. Lee, H.S. Cho, K.H. Kim, K.H. Choi, S.H. Lee, K.S. Song, C.S. Kang, I.J. Yu, Aspect ratio has no effect on genotoxicity of multi-wall carbon nanotubes, Arch. Toxicol. 85 (7) (2011) 775–786, http://dx.doi.org/10.1007/s00204-010-0574-0.

[95] B.B. Manshian, G.J. Jenkins, P.M. Williams, C. Wright, A.R. Barron, A.P. Brown, N. Hondow, P.R. Dunstan, R. Rickman, K. Brady, S.H. Doak, Single-walled carbon nanotubes: differential genotoxic potential associated with physico-chemical properties, Nanotoxicology 7 (2) (2013) 144–156, http://dx.doi.org/10.3109/17435390.2011.647928.

[96] J. Meng, X. Cheng, J. Liu, W. Zhang, X. Li, H. Kong, H. Xu, Effects of long and short carboxylated or aminated multiwalled carbon nanotubes on blood coagulation, PLoS One 7 (7) (2012), e38995 http://dx.doi.org/10.1371/journal.pone.0038995.

[97] L. Tabet, C. Bussy, A. Setyan, A. Simon-Deckers, M.J. Rossi, J. Boczkowski, S. Lanone, Coating carbon nanotubes with a polystyrene-based polymer protects against pulmonary toxicity, Part. Fibre Toxicol. 8 (2011) 3, http://dx.doi.org/10.1186/1743-8977-8-3.

[98] R.P. Singh, M. Das, V. Thakare, S. Jain, Functionalization density dependent toxicity of oxidized multiwalled carbon nanotubes in a murine macrophage cell line, Chem. Res. Toxicol. 25 (10) (2012) 2127–2137, http://dx.doi.org/10.1021/tx300228d (Erratum in: Chem Res Toxicol. 2012;25(11):2617).

[99] C.M. Sayes, F. Liang, J.L. Hudson, J. Mendez, W. Guo, J.M. Beach, V.C. Moore, C.D. Doyle, J.L. West, W.E. Billups, K.D. Ausman, V.L. Colvin, Functionalization density dependence of single-walled carbon nanotubes cytotoxicity in vitro, Toxicol. Lett. 161 (2) (2006) 135–142, http://dx.doi.org/10.1016/j.toxlet.2005.08.011.

[100] Y. Zhang, Y. Xu, Z. Li, T. Chen, S.M. Lantz, P.C. Howard, M.G. Paule, W. Slikker Jr., F. Watanabe, T. Mustafa, A.S. Biris, S.F. Ali, Mechanistic toxicity evaluation of uncoated and PEGylated single-walled carbon nanotubes in neuronal PC12 cells, ACS Nano 5 (9) (2011) 7020–7033, http://dx.doi.org/10.1021/nn2016259.

[101] K. Pulskamp, S. Diabaté, H.F. Krug, Carbon nanotubes show no sign of acute toxicity but induce intracellular reactive oxygen species in dependence on contaminants, Toxicol. Lett. 168 (1) (2007) 58–74, http://dx.doi.org/10.1016/j.toxlet.2006.11.001.

[102] A.A. Shvedova, V. Castranova, E.R. Kisin, D. Schwegler-Berry, A.R. Murray, V.Z. Gandelsman, A. Maynard, P. Baron, Exposure to carbon nanotube material: assessment of nanotube cytotoxicity using human keratinocyte cells, J. Toxicol. Environ. Health A 66 (20) (2003) 1909–1926, http://dx.doi.org/10.1080/713853956.

[103] W. Huang, Y. Wang, G. Luo, F. Wei, 99.9% purity multi-walled carbon nanotubes by vacuum high-temperature annealing, Carbon 41 (13) (2003) 2585–2590, http://dx.doi.org/10.1016/S0008-6223(03)00330-0.

[104] Y. Li, X. Zhang, J. Luo, W. Huang, J. Cheng, Purification of CVD synthesized single-wall carbon nanotubes by different acid oxidation treatments, Nanotechnology 15 (11) (2004) 1645.

[105] S. Fiorito, A. Serafino, F. Andreola, P. Bernier, Effects of fullerenes and single-wall carbon nanotubes on murine and human macrophages, Carbon 44 (6) (2006) 1100–1105, http://dx.doi.org/10.1016/j.carbon.2005.11.009.

[106] S. Hirano, S. Kanno, A. Furuyama, Multi-walled carbon nanotubes injure the plasma membrane of macrophages, Toxicol. Appl. Pharmacol. 232 (2) (2008) 244–251, http://dx.doi.org/10.1016/j.taap.2008.06.016.

[107] X. He, S.H. Young, D. Schwegler-Berry, W.P. Chisholm, J.E. Fernback, Q. Ma, Multiwalled carbon nanotubes induce a fibrogenic response by stimulating reactive oxygen species production, activating NF-κB signaling, and promoting fibroblast-to-myofibroblast transformation, Chem. Res. Toxicol. 24 (12) (2011) 2237–2248, http://dx.doi.org/10.1021/tx200351d.

[108] L. Tabet, C. Bussy, N. Amara, A. Setyan, A. Grodet, M.J. Rossi, J.C. Pairon, J. Boczkowski, S. Lanone, Adverse effects of industrial multiwalled carbon nanotubes on human pulmonary cells, J. Toxicol. Environ. Health A 72 (2) (2009) 60–73, http://dx.doi.org/10.1080/15287390802476991.

[109] H. Nagai, Y. Okazaki, S.H. Chew, N. Misawa, Y. Yamashita, S. Akatsuka, T. Ishihara, K. Yamashita, Y. Yoshikawa, H. Yasui, L. Jiang, H. Ohara, T. Takahashi, G. Ichihara, K. Kostarelos, Y. Miyata, H. Shinohara, S. Toyokuni, Diameter and rigidity of multiwalled carbon nanotubes are critical factors in mesothelial injury and carcinogenesis, Proc. Natl. Acad. Sci. U. S. A. 108 (49) (2011) E1330–E1338, http://dx.doi.org/10.1073/pnas.1110013108.

[110] X. Wang, G. Jia, H. Wang, H. Nie, L. Yan, X.Y. Deng, S. Wang, Diameter effects on cytotoxicity of multi-walled carbon nanotubes, J. Nanosci. Nanotechnol. 9 (5) (2009) 3025–3033.

[111] J.C. Charlier, Defects in carbon nanotubes, Acc. Chem. Res. 35 (12) (2002) 1063–1069, http://dx.doi.org/10.1021/ar010166k.

[112] I. Fenoglio, G. Greco, M. Tomatis, J. Muller, E. Raymundo-Piñero, F. Béguin, A. Fonseca, J.B. Nagy, D. Lison, B. Fubini, Structural defects play a major role in the acute lung toxicity of multiwall carbon nanotubes: physicochemical aspects, Chem. Res. Toxicol. 21 (9) (2008) 1690–1697, http://dx.doi.org/10.1021/tx800100s.

[113] J. Cheng, S.H. Cheng, Influence of carbon nanotube length on toxicity to zebrafish embryos, Int. J. Nanomedicine 7 (2012) 3731–3739, http://dx.doi.org/10.2147/IJN.S30459.

[114] O. Vittorio, V. Raffa, A. Cuschieri, Influence of purity and surface oxidation on cytotoxicity of multiwalled carbon nanotubes with human neuroblastoma cells, Nanomedicine 5 (4) (2009) 424–431, http://dx.doi.org/10.1016/j.nano.2009.02.006.

[115] C. Ge, J. Du, L. Zhao, L. Wang, Y. Liu, D. Li, Y. Yang, R. Zhou, Y. Zhao, Z. Chai, C. Chen, Binding of blood proteins to carbon nanotubes reduces cytotoxicity, Proc. Natl. Acad. Sci. U. S. A. 108 (41) (2011) 16968–16973, http://dx.doi.org/10.1073/pnas.1105270108.

[116] D. Dutta, S.K. Sundaram, J.G. Teeguarden, B.J. Riley, L.S. Fifield, J.M. Jacobs, S.R. Addleman, G.A. Kaysen, B.M. Moudgil, T.J. Weber, Adsorbed proteins influence the biological activity and molecular targeting of nanomaterials, Toxicol. Sci. 100 (1) (2007) 303–315, http://dx.doi.org/10.1093/toxsci/kfm217.

[117] R. Foldbjerg, E.S. Irving, J. Wang, K. Thorsen, D.S. Sutherland, H. Autrup, C. Beer, The toxic effects of single-walled carbon nanotubes are linked to the phagocytic ability of cells, Toxicol. Res. 3 (4) (2014) 228–241, http://dx.doi.org/10.1039/C3TX50099C.

[118] W. Asghar, H. Shafiee, V. Velasco, V.R. Sah, S. Guo, R. El Assal, F. Inci, A. Rajagopalan, M. Jahangir, R.M. Anchan, G.L. Mutter, M. Ozkan, C.S. Ozkan, U. Demirci, Toxicology study of single-walled carbon nanotubes and reduced graphene oxide in human sperm, Sci. Rep. 6 (2016) 30270, http://dx.doi.org/10.1038/srep30270.

[119] S.K. Manna, S. Sarkar, J. Barr, K. Wise, E.V. Barrera, O. Jejelowo, A.C. Rice-Ficht, G.T. Ramesh, Single-walled carbon nanotube induces oxidative stress and activates

nuclear transcription factor-kappaB in human keratinocytes, Nano Lett. 5 (9) (2005) 1676–1684, http://dx.doi.org/10.1021/nl0507966.
[120] J. Palomäki, E. Välimäki, J. Sund, M. Vippola, P.A. Clausen, K.A. Jensen, K. Savolainen, S. Matikainen, H. Alenius, Long, needle-like carbon nanotubes and asbestos activate the NLRP3 inflammasome through a similar mechanism, ACS Nano 5 (9) (2011) 6861–6870, http://dx.doi.org/10.1021/nn200595c.
[121] B.D. Holt, P.A. Short, A.D. Rape, Y.-l. Wang, M.F. Islam, K.N. Dahl, Carbon nanotubes reorganize actin structures in cells and ex vivo, ACS Nano 4 (2010) 4872–4878, http://dx.doi.org/10.1021/nn101151x.
[122] A. Takagi, A. Hirose, T. Nishimura, N. Fukumori, A. Ogata, N. Ohashi, S. Kitajima, J. Kanno, Induction of mesothelioma in p53+/− mouse by intraperitoneal application of multi-wall carbon nanotube, J. Toxicol. Sci. 33 (1) (2008) 105–116, http://dx.doi.org/10.2131/jts.33.105.
[123] L. Wang, S. Luanpitpong, V. Castranova, W. Tse, Y. Lu, V. Pongrakhananon, Y. Rojanasakul, Carbon nanotubes induce malignant transformation and tumorigenesis of human lung epithelial cells, Nano Lett. 11 (7) (2011) 2796–2803, http://dx.doi.org/10.1021/nl2011214.
[124] C. Salvador-Morales, E. Flahaut, E. Sim, J. Sloan, M.L. Green, R.B. Sim, Complement activation and protein adsorption by carbon nanotubes, Mol. Immunol. 43 (3) (2006) 193–201, http://dx.doi.org/10.1016/j.molimm.2005.02.006.
[125] K.M. Pondman, M. Sobik, A. Nayak, A.G. Tsolaki, A. Jäkel, E. Flahaut, S. Hampel, B. Ten Haken, R.B. Sim, U. Kishore, Complement activation by carbon nanotubes and its influence on the phagocytosis and cytokine response by macrophages, Nanomedicine 10 (6) (2014) 1287–1299, http://dx.doi.org/10.1016/j.nano.2014.02.010.
[126] X. Deng, F. Wu, Z. Liu, M. Luo, L. Li, Q. Ni, Z. Jiao, M. Wu, Y. Liu, The splenic toxicity of water soluble multi-walled carbon nanotubes in mice, Carbon 47 (2009) 1421–1428, http://dx.doi.org/10.1016/j.carbon.2008.12.032.
[127] G. Qu, Y. Bai, Y. Zhang, Q. Jia, W. Zhang, B. Yan, The effect of multiwalled carbon nanotube agglomeration on their accumulation in and damage to organs in mice, Carbon 47 (2009) 2060–2069, http://dx.doi.org/10.1016/j.carbon.2009.03.056.
[128] M.L. Schipper, N. Nakayama-Ratchford, C.R. Davis, N.W. Kam, P. Chu, Z. Liu, X. Sun, H. Dai, S.S. Gambhir, A pilot toxicology study of single-walled carbon nanotubes in a small sample of mice, Nat. Nanotechnol. 3 (4) (2008) 216–221, http://dx.doi.org/10.1038/nnano.2008.68.
[129] S. Tang, Y. Tang, L. Zhong, K. Murat, G. Asan, J. Yu, R. Jian, C. Wang, P. Zhou, Short- and long-term toxicities of multi-walled carbon nanotubes in vivo and in vitro, J. Appl. Toxicol. 32 (11) (2012) 900–912, http://dx.doi.org/10.1002/jat.2748.
[130] Z. Ji, D. Zhang, L. Li, X. Shen, X. Deng, L. Dong, M. Wu, Y. Liu, The hepatotoxicity of multi-walled carbon nanotubes in mice, Nanotechnology 20 (44) (2009) 445101, http://dx.doi.org/10.1088/0957-4484/20/44/445101.
[131] X. Wang, R. Podila, J.H. Shannahan, A.M. Rao, J.M. Brown, Intravenously delivered graphene nanosheets and multiwalled carbon nanotubes induce site-specific Th2 inflammatory responses via the IL-33/ST2 axis, Int. J. Nanomedicine 8 (2013) 1733–1748, http://dx.doi.org/10.2147/IJN.S44211.
[132] S. Jain, V.S. Thakare, M. Das, C. Godugu, A.K. Jain, R. Mathur, K. Chuttani, A.K. Mishra, Toxicity of multiwalled carbon nanotubes with end defects critically depends on their functionalization density, Chem. Res. Toxicol. 24 (11) (2011) 2028–2039, http://dx.doi.org/10.1021/tx2003728.
[133] S.T. Yang, X. Wang, G. Jia, Y. Gu, T. Wang, H. Nie, C. Ge, H. Wang, Y. Liu, Long-term accumulation and low toxicity of single-walled carbon nanotubes in intravenously exposed mice, Toxicol. Lett. 181 (3) (2008) 182–189, http://dx.doi.org/10.1016/j.toxlet.2008.07.020.
[134] B. Han, M. Zhang, T. Tang, Q. Zheng, K. Wang, L. Li, W. Chen, The long-term fate and toxicity of PEG-modified single-walled carbon nanotube isoliquiritigenin delivery vehicles in rats, J. Nanomater. 2014 (257391) (2014) 1–8, http://dx.doi.org/10.1155/2014/257391.
[135] A. Al Faraj, F. Fauvelle, N. Luciani, G. Lacroix, M. Levy, Y. Crémillieux, E. Canet-Soulas, In vivo biodistribution and biological impact of injected carbon nanotubes using magnetic resonance techniques, Int. J. Nanomedicine 6 (2011) 351–361, http://dx.doi.org/10.2147/IJN.S16653.
[136] Z. Liu, C. Davis, W. Cai, L. He, X. Chen, H. Dai, Circulation and long-term fate of functionalized, biocompatible single-walled carbon nanotubes in mice probed by Raman spectroscopy, Proc. Natl. Acad. Sci. U. S. A. 105 (5) (2008) 1410–1415, http://dx.doi.org/10.1073/pnas.0707654105.
[137] D. Zhao, D. Alizadeh, L. Zhang, W. Liu, O. Farrukh, E. Manuel, D.J. Diamond, B. Badie, Carbon nanotubes enhance CpG uptake and potentiate antiglioma immunity, Clin. Cancer Res. 17 (4) (2011) 771–782, http://dx.doi.org/10.1158/1078-0432.CCR-10-2444.
[138] T. Santos, X. Fang, M.T. Chen, W. Wang, R. Ferreira, N. Jhaveri, M. Gundersen, C. Zhou, P. Pagnini, F.M. Hofman, T.C. Chen, Sequential administration of carbon nanotubes and near-infrared radiation for the treatment of gliomas, Front. Oncol. 4 (2014) 180, http://dx.doi.org/10.3389/fonc.2014.00180.
[139] S.U. Moon, J. Kim, K.K. Bokara, J.Y. Kim, D. Khang, T.J. Webster, J.E. Lee, Carbon nanotubes impregnated with subventricular zone neural progenitor cells promotes recovery from stroke, Int. J. Nanomedicine 7 (2012) 2751–2765, http://dx.doi.org/10.2147/IJN.S30273.
[140] H.J. Lee, J. Park, O.J. Yoon, H.W. Kim, D.Y. Lee, d.H. Kim, L. WB, L. NE, B. JV, K. SS, Amine-modified single-walled carbon nanotubes protect neurons from injury in a rat stroke model, Nat. Nanotechnol. 6 (2) (2011) 121–125, http://dx.doi.org/10.1038/nnano.2010.281.
[141] X. Xue, J.Y. Yang, Y. He, L.R. Wang, P. Liu, L.S. Yu, G.H. Bi, M.M. Zhu, Y.Y. Liu, R.W. Xiang, X.T. Yang, X.Y. Fan, X.M. Wang, J. Qi, H.J. Zhang, T. Wei, W. Cui, G.L. Ge, Z.X. Xi, C.F. Wu, X.J. Liang, Aggregated single-walled carbon nanotubes attenuate the behavioural and neurochemical effects of methamphetamine in mice, Nat. Nanotechnol. 11 (7) (2016) 613–620, http://dx.doi.org/10.1038/nnano.2016.23.
[142] K.T. Al-Jamal, L. Gherardini, G. Bardi, A. Nunes, C. Guo, C. Bussy, M.A. Herrero, A. Bianco, M. Prato, K. Kostarelos, T. Pizzorusso, Functional motor recovery from brain ischemic insult by carbon nanotube-mediated siRNA silencing, Proc. Natl. Acad. Sci. U. S. A. 108 (27) (2011) 10952–10957, http://dx.doi.org/10.1073/pnas.1100930108.
[143] A. Patabendige, R.A. Skinner, N.J. Abbott, Establishment of a simplified in vitro porcine blood-brain barrier model with high transendothelial electrical resistance, Brain Res. 1521 (2013) 1–15, http://dx.doi.org/10.1016/j.brainres.2012.06.057.
[144] H. Kafa, J.T. Wang, N. Rubio, K. Venner, G. Anderson, E. Pach, B. Ballesteros, J.E. Preston, N.J. Abbott, K.T. Al-Jamal, The interaction of carbon nanotubes with an in vitro blood-brain barrier model and mouse brain in vivo, Biomaterials 53 (2015) 437–452, http://dx.doi.org/10.1016/j.biomaterials.2015.02.083.
[145] H. Kafa, J.T. Wang, N. Rubio, R. Klippstein, P.M. Costa, H.A. Hassan, J.K. Sosabowski, S.S. Bansal, J.E. Preston, N.J. Abbott, K.T. Al-Jamal, Translocation of LRP1 targeted carbon nanotubes of different diameters across the blood-brain barrier in vitro and in vivo, J. Control. Release 225 (2016) 217–229, http://dx.doi.org/10.1016/j.jconrel.2016.01.031.
[146] S. Shityakov, E. Salvador, G. Pastorin, C. Förster, Blood-brain barrier transport studies, aggregation, and molecular dynamics simulation of multiwalled carbon nanotube functionalized with fluorescein isothiocyanate, Int. J. Nanomedicine 10 (2015) 1703–1713, http://dx.doi.org/10.2147/IJN.S68429.
[147] M. Demeule, A. Régina, C. Ché, J. Poirier, T. Nguyen, R. Gabathuler, J.P. Castaigne, R. Béliveau, Identification and design of peptides as a new drug delivery system for the brain, J. Pharmacol. Exp. Ther. 324 (3) (2008) 1064–1072, http://dx.doi.org/10.1124/jpet.107.131318.
[148] J.T. Wang, C. Fabbro, E. Venturelli, C. Ménard-Moyon, O. Chaloin, T. Da Ros, L. Methven, A. Nunes, J.K. Sosabowski, S.J. Mather, M.K. Robinson, J. Amadou, M. Prato, A. Bianco, K. Kostarelos, K.T. Al-Jamal, The relationship between the diameter of chemically-functionalized multi-walled carbon nanotubes and their organ biodistribution profiles in vivo, Biomaterials 35 (35) (2014) 9517–9528, http://dx.doi.org/10.1016/j.biomaterials.2014.07.054.
[149] J.T. Wang, N. Rubio, H. Kafa, E. Venturelli, C. Fabbro, C. Ménard-Moyon, T. Da Ros, J.K. Sosabowski, A.D. Lawson, M.K. Robinson, M. Prato, A. Bianco, F. Festy, J.E. Preston, K. Kostarelos, K.T. Al-Jamal, Kinetics of functionalised carbon nanotube distribution in mouse brain after systemic injection: spatial to ultra-structural analyses, J. Control. Release 224 (2016) 22–32, http://dx.doi.org/10.1016/j.jconrel.2015.12.039.
[150] Z. Yang, Y. Zhang, Y. Yang, L. Sun, D. Han, H. Li, C. Wang, Pharmacological and toxicological target organelles and safe use of single-walled carbon nanotubes as drug carriers in treating Alzheimer disease, Nanomedicine 6 (3) (2010) 427–441, http://dx.doi.org/10.1016/j.nano.2009.11.007.
[151] J. Ren, S. Shen, D. Wang, Z. Xi, L. Guo, Z. Pang, Y. Qian, X. Sun, X. Jiang, The targeted delivery of anticancer drugs to brain glioma by PEGylated oxidized multi-walled carbon nanotubes modified with angiopep-2, Biomaterials 33 (11) (2012) 3324–3333, http://dx.doi.org/10.1016/j.biomaterials.2012.01.025.
[152] N.M. Iverson, P.W. Barone, M. Shandell, L.J. Trudel, S. Sen, F. Sen, V. Ivanov, E. Atolia, E. Farias, T.P. McNicholas, N. Reuel, N.M. Parry, G.N. Wogan, M.S. Strano, In vivo biosensing via tissue-localizable near-infrared-fluorescent single-walled carbon nanotubes, Nat. Nanotechnol. 8 (11) (2013) 873–880, http://dx.doi.org/10.1038/nnano.2013.222.
[153] G. Bardi, P. Tognini, G. Ciofani, V. Raffa, M. Costa, T. Pizzorusso, Pluronic-coated carbon nanotubes do not induce degeneration of cortical neurons in vivo and in vitro, Nanomedicine 5 (1) (2009) 96–104, http://dx.doi.org/10.1016/j.nano.2008.06.008.
[154] G. Bardi, A. Nunes, L. Gherardini, K. Bates, K.T. Al-Jamal, C. Gaillard, M. Prato, A. Bianco, T. Pizzorusso, K. Kostarelos, Functionalized carbon nanotubes in the brain: cellular internalization and neuroinflammatory responses, PLoS One 8 (11) (2013), e80964 http://dx.doi.org/10.1371/journal.pone.0080964.
[155] C. Bussy, K.T. Al-Jamal, J. Boczkowski, S. Lanone, M. Prato, A. Bianco, K. Kostarelos, Microglia determine brain region-specific neurotoxic responses to chemically functionalized carbon nanotubes, ACS Nano 9 (8) (2015) 7815–7830, http://dx.doi.org/10.1021/acsnano.5b02358.
[156] K. Bhattacharya, C. Sacchetti, R. El-Sayed, A. Fornara, G.P. Kotchey, J.A. Gaugler, A. Star, M. Bottini, B. Fadeel, Enzymatic 'stripping' and degradation of PEGylated carbon nanotubes, Nanoscale 6 (24) (2014) 14686–14690, http://dx.doi.org/10.1039/c4nr03604b.
[157] S.T. Yang, H. Wang, M.J. Meziani, Y. Liu, X. Wang, Y.P. Sun, Biodefunctionalization of functionalized single-walled carbon nanotubes in mice, Biomacromolecules 10 (7) (2009) 2009–2012, http://dx.doi.org/10.1021/bm900263z.